

Sensitivity Analysis of a Space-borne Gravitational Wave Detector

by

Midshipman 1/C Drew R. Barker, Class of 2004
United States Naval Academy
Annapolis, Maryland

(signature)

(date)

Dr. Richard P. Fahey
Aerospace Engineering Department

(signature)

(date)

Professor Lawrence L. Tankersley
Physics Department

(signature)

(date)

Acceptance for the Trident Scholar Committee

Professor Joyce E. Shade
Deputy Director of Research and Scholarship

(signature)

(date)

REPORT DOCUMENTATION PAGE			Form Approved OMB No. 074-0188	
Public reporting burden for this collection of information is estimated to average 1 hour per response, including the time for reviewing instructions, searching existing data sources, gathering and maintaining the data needed, and completing and reviewing the collection of information. Send comments regarding this burden estimate or any other aspect of the collection of information, including suggestions for reducing this burden to Washington Headquarters Services, Directorate for Information Operations and Reports, 1215 Jefferson Davis Highway, Suite 1204, Arlington, VA 22202-4302, and to the Office of Management and Budget, Paperwork Reduction Project (0704-0188), Washington, DC 20503.				
1. AGENCY USE ONLY (Leave blank)		2. REPORT DATE 5 May 2004		3. REPORT TYPE AND DATE COVERED
4. TITLE AND SUBTITLE Sensitivity analysis of a space-borne gravitational wave detector			5. FUNDING NUMBERS	
6. AUTHOR(S) Barker, Drew R. (Drew Richard), 1982-				
7. PERFORMING ORGANIZATION NAME(S) AND ADDRESS(ES)			8. PERFORMING ORGANIZATION REPORT NUMBER	
9. SPONSORING/MONITORING AGENCY NAME(S) AND ADDRESS(ES) US Naval Academy Annapolis, MD 21402			10. SPONSORING/MONITORING AGENCY REPORT NUMBER Trident Scholar project report no. 318 (2004)	
11. SUPPLEMENTARY NOTES				
12a. DISTRIBUTION/AVAILABILITY STATEMENT This document has been approved for public release; its distribution is UNLIMITED.				12b. DISTRIBUTION CODE
13. ABSTRACT: Modern theories of gravity predict ripples in space and time, which are known as gravitational waves. Very large interacting masses, such as binary systems of neutron stars or black holes, are predicted to generate gravitational waves that may be intense enough to be detected. This study presents a response analysis for the proposed gravitational wave experiment known as the Laser Interferometer Space Antenna (LISA). The analysis focuses on the gravitational wave distortion patterns, or polarizations, predicted by the Brans-Dicke Scalar-Tensor Theory of Gravity (BD). LISA, a cooperative venture between the National Aeronautics and Space Administration (NASA) and the European Space Agency (ESA), is a proposed space-based gravitational wave experiment with the potential to distinguish between polarizations of gravitational waves. LISA is scheduled for launch in 2012; so much of the current work for LISA involves the development and design of systems and procedures that will allow LISA to attain its desired performance. For a gravitational wave experiment, the projected sensitivity is determined by an instrument response function, which relates the disturbance generated by the gravitational wave to the disturbance that can be measured by the instrument. This study compares the response functions for BD polarizations to the published response functions for GR. Response functions co-responding to several different methods of data collection were analyzed. To numerically evaluate and compare the response functions, two programs were generated in the MATLAB® programming language. The first program computes the response functions averaged over all source directions for each gravitational wave polarization and data collection method. The second program calculates the instrument response at each point in LISA's orbit to gravitational waves originating from the galactic center. The results from the programs generated in Matlab identify patterns in the response functions that distinguish between gravitational waves of BD and GR polarizations. These results identify features of the response functions that may assist future researchers in determining the optimal data collection method to detect gravitational waves of a given polarization, frequency, and source direction.				
14. SUBJECT TERMS: Brans-Dicke, experimental relativity, gravitational wave, gravitational radiation, Laser Interferometer Space Antenna, LISA			15. NUMBER OF PAGES 59	
			16. PRICE CODE	
17. SECURITY CLASSIFICATION OF REPORT		18. SECURITY CLASSIFICATION OF THIS PAGE		19. SECURITY CLASSIFICATION OF ABSTRACT
				20. LIMITATION OF ABSTRACT

Abstract

Modern theories of gravity predict ripples in space and time, which are known as gravitational waves. Very large interacting masses, such as binary systems of neutron stars or black holes, are predicted to generate gravitational waves that may be intense enough to be detected. This study presents a response analysis for the proposed gravitational wave experiment known as the Laser Interferometer Space Antenna (LISA). The analysis focuses on the gravitational wave distortion patterns, or polarizations, predicted by the Brans-Dicke Scalar-Tensor Theory of Gravity (BD). Several plausible metric theories of gravity, such as BD, predict gravitational wave polarizations that differ from the traditionally expected polarizations predicted by General Relativity (GR). LISA, a cooperative venture between the National Aeronautics and Space Administration (NASA) and the European Space Agency (ESA), is a proposed space-based gravitational wave experiment with the potential to distinguish between polarizations of gravitational waves. LISA is scheduled for launch in 2012; so much of the current work for LISA involves the development and design of systems and procedures that will allow LISA to attain its desired performance.

For a gravitational wave experiment, the projected sensitivity is determined by an instrument response function, which relates the disturbance generated by the gravitational wave to the disturbance that can be measured by the instrument. This study compares the response functions for BD polarizations to the published response functions for GR. Response functions corresponding to several different methods of data collection were analyzed. The analysis revealed that each response function depends strongly on the polarization, frequency, and propagation direction of the gravitational wave.

To numerically evaluate and compare the response functions two programs were generated in the MATLAB® programming language. The first program computes the response functions averaged over all source directions for each gravitational wave polarization and data collection method. The second program calculates the instrument response at each point in LISA's orbit to gravitational waves originating from the galactic center. The results from the programs generated in Matlab identify patterns in the response functions that distinguish between gravitational waves of BD and GR polarizations. These results identify features of the response functions that may assist future researchers in determining the optimal data collection method to detect gravitational waves of a given polarization, frequency, and source direction.

Acknowledgements

Many thanks to both of my advisors, Dr. Fahey and Dr. Tankersley, for the invaluable time and effort they have put into my personal and professional development through this project. Dr. Stephen Merkowitz served as an external collaborator from Goddard Space Flight Center in Greenbelt, MD, providing both insight and direction. Dr. John Pierce of the Math Department aided with the Matlab debugging process, and Dr. Konkowski provided insights into the mathematics of General Relativity.

Table of Contents

Abstract	1
Acknowledgements	2
Table of Contents	3
Introduction	4
Methods	16
Results	25
Conclusions	37
Appendix A	38
Appendix B	42
Appendix C	51
References	58

Introduction

The discovery and analysis of gravitational waves promises to usher in a new age of astronomy. Nearly all astronomical data are gathered from electromagnetic radiation emitted by accelerated electrical charges in distant stars. The detection and subsequent analysis of radiation emitted by accelerated mass would provide a new probe of the universe and its structure.

The apparent parallels between the gravitational interaction and the electromagnetic force have long been recognized. The most obvious parallel is the similarity between Isaac Newton's Law of Universal Gravitation and Charles Coulomb's Electrostatic Force Law:

$$F_g = \frac{Gm_1m_2}{r^2} \quad (1)$$

$$F_e = \frac{kq_1q_2}{r^2} \quad (2)$$

Both equations involve a constant (G or k) multiplied by a fundamental quantity (mass and charge) of two objects, and divided by the distance separating the objects squared. Until the 20th century, no one considered searching for a gravitational radiation similar to electromagnetic radiation but generated by the acceleration of mass. Because Newton's theory of gravity fails to support the wave equation necessary for the existence of gravitational radiation, a search for gravitational radiation was not merited until the general theory of relativity was published in 1915 [1].

In Newton's theory, gravity is considered to be a force that is experienced instantaneously, that is to say that if the Sun were to suddenly vanish, the earth and all the other

planets would immediately depart their orbits and head for deep space with the velocity they had the moment the sun vanished. Einstein departed from the instantaneous gravitational effect intrinsic to Newton's theory by assuming that no information, including the gravitational interaction, could propagate faster than the speed of light in vacuum, which he assumed as invariant [2].

Einstein thoroughly explored the consequences of assuming the speed of light to be a constant, and published the results of his investigation in 1905 in his Special Theory of Relativity [1]. Special relativity allows one to find the relationship between measurements made in two inertial reference frames. To illustrate the concept of special relativity (See Fig. 1), consider a situation where Bob stands on a flatbed railcar with a timepiece that consists of light that bounces between two mirrors.

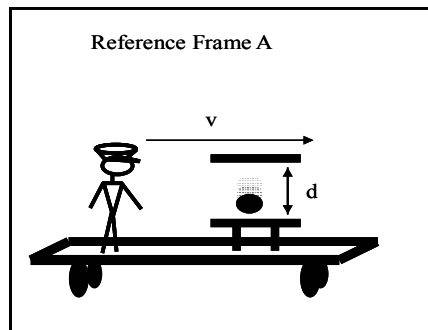


Figure 1: In reference frame A, Bob observes a timepiece consisting of a photon bouncing between two mirrors.

Light has the special property that it travels through space at a constant rate (c) that does not depend on the motion of the source or receiver. As the light completes one round trip, Bob (in reference frame A) will observe the light traveling a distance $2d$ in the time t ,

where $t = 2d/c$. Meanwhile, in reference frame B, Alice stands on the ground and watches the flatbed car travel by her at a velocity v (See Fig. 2).

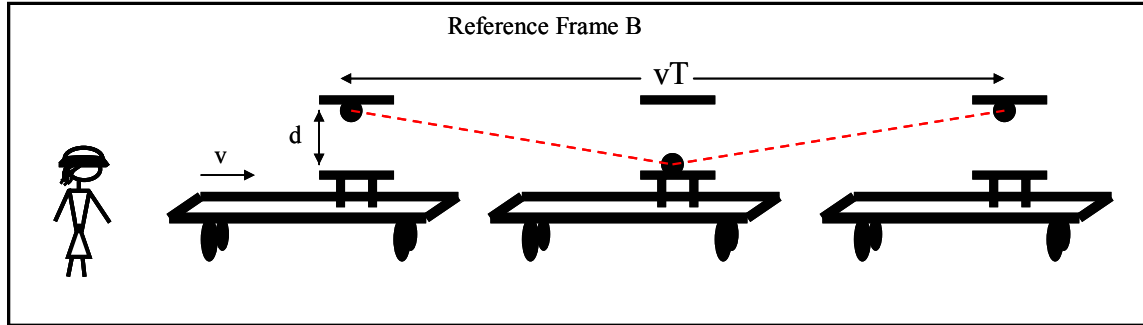


Figure 2: In reference frame B, Alice observes the path taken by a photon traveling between two mirrors that are moving relative to her position.

Alice observes the light traveling a distance greater than $2d$ as it makes a round trip. Consequently, she notices **more time** has elapsed between **the same two events** that Bob witnessed in Reference Frame A. Though the amount of time observed between two events is dependent upon the reference frame, Einstein concluded that the right mixture of space and time, referred to as the spacetime interval, does not depend upon the reference frame. The spacetime interval and the principle that there is no preferred frame or observer are the essence of special relativity. The invariant interval is given by the equation:

$$\Delta s^2 = \Delta x^2 + \Delta y^2 + \Delta z^2 - \Delta(ct)^2. \quad (3)$$

Therefore, light in all reference frames propagates between spacetime points separated by a null interval ($\Delta s^2 = 0$). Special relativity is only valid for reference frames that are moving at

constant velocities and does not account for gravitational effects. In order to apply the precepts of relativity to a gravitational context, Einstein used what is called the equivalence principle [2]. To begin, Einstein surmised that the effects of gravity were no different than the effects experienced in an accelerated reference frame. For example, consider the two reference frames illustrated in Fig. 3.

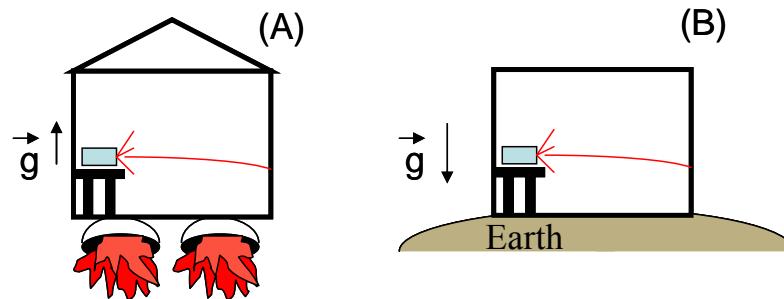


Figure 3: A rocket ship blasts upwards so an observer would witness laser light inside the spacecraft following a curved line (A). The acceleration due to the gravitation of the earth causes light to bend in the same manner as seen on an accelerating spacecraft (B).

The two reference frames consist of identical rooms; one room located on a spacecraft accelerating upwards at 9.8 m/s^2 and the other room located at the surface of the earth where the gravity causes a free fall acceleration of 9.8 m/s^2 . In both rooms a laser at the left end of the room shoots a beam that hits the right side of the room. Because the rocket in reference frame A accelerates up during the time the laser light travels across the room, the path of the light appears to bend so that it impacts the wall on the right side of the room at a point lower than the initial height of the laser. The equivalence principle asserts that a gravitational field will have the same effect on the laser beam. Einstein realized that the path taken by the laser could be described by a geodesic curve in spacetime. He was then able to create the general theory of relativity by developing equations that describe how matter influences the geometry of spacetime while the

geometry of spacetime influences the motion of matter [1]. The equations Einstein developed, known as field equations, are analogous to Maxwell's equations for electromagnetism, and they predict the wave equation that Newton's theory did not support.

Because Einstein's theory describes gravity in terms of the geometry of spacetime, it is referred to as a metric theory of gravity. After studying Einstein's approach to gravity, several other scientists have developed alternative metric theories that describe the connection between matter and spacetime curvature differently. In the 1960's Carl Brans and Robert Dicke published a scalar-tensor theory of gravity [3]. The Brans-Dicke theory (BD) was developed to incorporate Mach's principle into Einstein's theory of gravity. Mach's principle asserts that the inertial properties of matter are dependent upon the total distribution of matter in the universe [3]. The essential result of BD is that the gravitational "constant" G is not constant, but dependent upon the totality of matter in the universe and can vary from place to place and time to time [3]. In general, BD and other alternative theories agree with the results of GR when the gravitational field is relatively weak, such as within the solar system. However, as the gravitational field becomes stronger, the mathematical description of spacetime curvature becomes increasingly complicated, and the predictions of alternative theories diverge from the predictions of GR [4]. Gravitational waves with sufficient amplitude for detection are only created within the strongest gravitational fields. As a gravitational wave leaves the strong field, the persisting polarization and frequency of the wave contains information on the nature of the strong field produced by the source. Because it is not possible to send a gravitational experiment to the surface of a distant neutron star or black hole where the gravitational field is recognized as strong, the properties of the gravitational interaction in the strong field are not well known. The detection and analysis of gravitational waves may be the first test to validate theories that differ

from GR only in the limit of the strong field [5]. Gravitational wave detection stands as the long awaited window into the nature of the strongest gravitational fields.

Theoretically, gravitational waves originate with any acceleration of mass; however, due to the weak nature of the gravitational interaction, only the most intense accelerations of the densest matter will result in gravitational waves that may be measurable [6]. Binary systems of neutron stars or black holes are likely to produce gravitational waves of sufficient strength to measure [7]. Gravitational waves act to stretch or shrink the space that they travel through in predictable patterns. Consequently, objects in the path of a gravitational wave will experience a compressive or tensile strain, and the distances between objects will either decrease or increase. Strain is measured by the change in length over the original length ($\Delta L/L$). The distortion pattern, or polarization, of the gravitational wave determines the direction an object will be strained, and similarly the direction objects will move in relation to one another. GR predicts two polarizations, which are known as the plus and cross polarizations [8]. In addition to the two polarizations predicted by GR, BD predicts the existence of a third polarization, designated here as the scalar polarization [6]. All three polarizations cause spatial strains that are transverse relative to the direction of propagation. Figure 4 depicts how a gravitational wave with a plus polarization would affect a group of masses arranged in a circle. The distortion pattern is mapped out over one period in the gravitational wave.

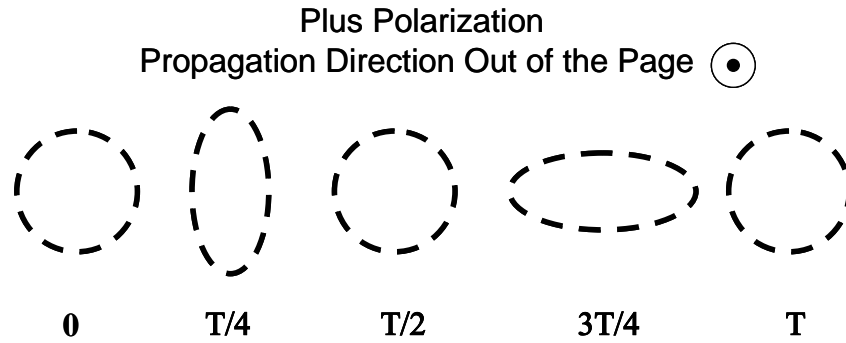


Figure 4: The strain pattern exhibited by the plus polarization in one cycle of a gravitational wave illustrated in a series of snapshots. The numbers below each snapshot indicate the progression of the gravitational wave through a single cycle - zero indicates the beginning of a cycle and T indicates the end of the cycle. [6]

The cross polarization behaves similarly although the strain pattern is rotated by 45 degrees about the direction of propagation.

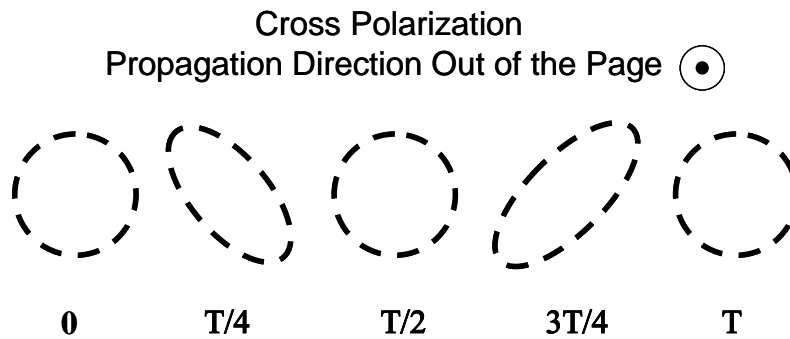


Figure 5: The strain pattern exhibited by the cross polarization through one cycle. [6]

Finally, the scalar polarization acts as a breathing mode causing a tensile strain in all transverse directions followed in time by a compressive strain.

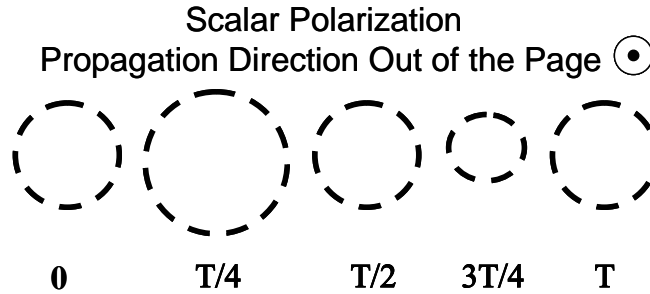


Figure 6: The strain pattern exhibited by the scalar polarization through one cycle. [6]

The illustrations of the three polarizations are helpful to visualize the strain pattern of a gravitational wave; however, they in no way indicate the amplitude of the wave. Known systems of binary neutron stars are predicted to produce gravitational waves that will reach earth with a strain amplitude, a fractional change in length over length, on the order of 10^{-21} [7], which is the approximate design sensitivity for LISA. Such a gravitational wave will change the length of a thousand kilometer ruler by about the diameter of a proton. Two approaches have been explored to detect such a small strain. The first involves a solid aluminum bar designed to “ring” when a gravitational wave with a particular frequency travels through it. If the aluminum bar’s fundamental mode of vibration has a frequency that matches that of the gravitational wave, then each passing phase of the gravitational wave will add to the vibrational energy of the bar in a resonance effect. The resulting vibrational strain in the bar could, in theory, be several orders of magnitude greater than the amplitude of the incident wave. However, no bar detector has verifiably detected a gravitational wave [9].

The second approach uses lasers to measure changes in the distance between points in space that are marked off by proof masses. The proof masses can be thought of as points on the circles used to illustrate the different polarizations. For ground based experiments the proof masses define points at the end of arms that are mutually perpendicular to one another (See Fig. 7).

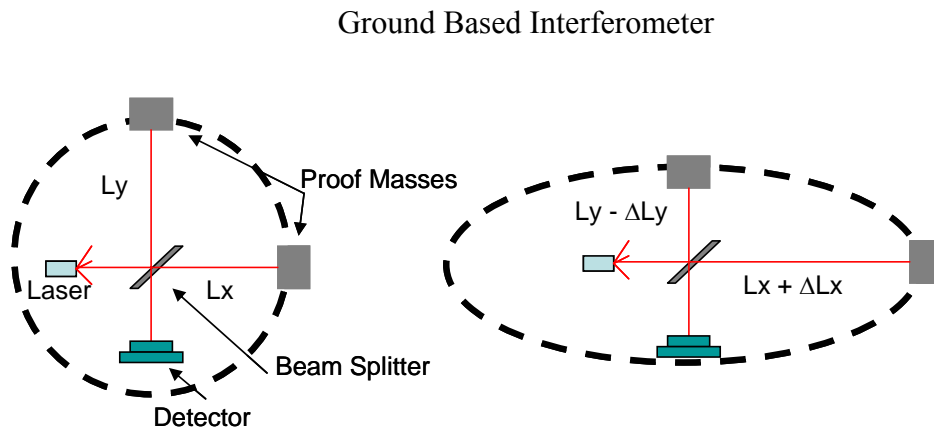


Figure 7: A depiction of an earth based gravitational wave interferometer. As the gravitational wave warps the space containing the interferometer the lengths of the respective arms will shrink or grow by an amount dictated by the amplitude, polarization, and propagation direction of the gravitational wave. [9]

A laser beam is sent through a beam splitter and directed down two paths that are equal in length (L_x and L_y). This setup will be referred to in this report as the two-arm Michelson mode of detection. The beams reflect off the proof masses and recombine at the beam splitter where they are directed to a detector. The intensity of the light measured at the detector is related to the difference in the lengths of each arm, $|L_x - L_y|$. If both paths are exactly equal in length then the beams will destructively interfere and the detector will measure an intensity minimum. If one path is longer than the other by half of the wavelength of the laser light, then the beams will constructively interfere and the detector will measure an intensity maximum. The shift from an

intensity minimum to maximum is known as one-half of an interference fringe shift. The ground based interferometer experiments are limited by the length of the arms (approximately 4 km) and by seismic noise which disturbs the instrument causing false signals [9]. A similar interferometer built in space could have arm lengths nearly 500 times the diameter of the earth and would not be subject to seismic noise [7].

The design and construction of a space-borne interferometer known as the Laser Interferometer Space Antenna (LISA) is currently being led by the National Aeronautics and Space Administration's Goddard Space Flight Center. In the LISA design, spacecraft will occupy the vertices of an equilateral triangle 5 million kilometers on a side. The significant increase in path length reduces the fractional change necessary to give a fringe shift. As a result, the effective detection band is shifted to lower frequencies. LISA is designed for the 10^{-4} to 10^0 Hertz band. The triangle will follow the earth in its orbit and will rotate clockwise as it revolves around the sun [7] (See Fig. 8).

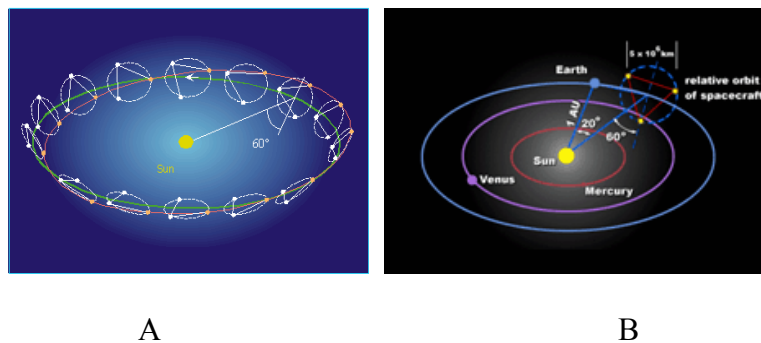


Figure 8: These pictures illustrate the LISA configuration. Picture A illustrates how each spacecraft follows its own orbit about the sun so that the three spacecraft will maintain relative positions at the vertices of an equilateral triangle throughout the course of a complete revolution about the sun. Picture B shows the location of the LISA configuration relative to the earth's orbit [10].

Each spacecraft contains a laser and proof masses so the constellation of three spacecraft can operate as one instrument on the same principle as the ground based experiments. Because each spacecraft in the LISA setup contains an interferometer, the data gathered from the fringe shifts measured at the detectors can be related to several different combinations of the arm lengths [11].

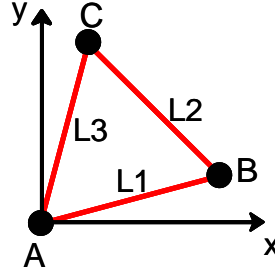


Figure 9: The LISA reference frame defined in this study. $L1$, $L2$, and $L3$ represent the lengths of each arm.

For example, in reference to Fig. 9, spacecraft A will collect data corresponding to $|L1 - L3|$, while spacecraft B will collect data corresponding to $|L1 - L2|$, and so on. Data transmitted to earth can be reprocessed to yield other combinations including permutations of $|L1 + L2 - 2L3|$ and $|L1 + L2 + L3|$ [11]. The different kinds of combinations will be referred to in this paper as modes of data collection. Four modes of data collection are examined in this study. The first mode evaluates the response of a single arm, the second computes the LISA equivalent to the two-arm Michelson mode that is used in earth based detectors. The two arm Michelson is defined by $|L1 - L2|$. The third mode is a result of combining the results of two independent two arm Michelson responses. It is referred to as the three-arm Michelson mode and is defined by $|L1 + L2 - 2L3|$. The final mode utilizes the LISA setup as a Sagnac interferometer so it is appropriately titled the Sagnac mode and is designated as $|L1 + L2 + L3|$.

Determining the sensitivity of each mode of data collection to gravitational waves of various frequencies, source directions and polarizations is an essential part of the LISA program. Several groups have published studies of LISA's sensitivity to the gravitational wave polarizations predicted by GR [7, 11, 12]. Other groups have reported that no experiment to date provides data to exclude scalar-tensor theories like BD. The following report is the first to explore the response of LISA to the additional gravitational wave polarization predicted by BD.

Methods

The sensitivity of LISA can be calculated through a combination of two functions; a noise function and a response function. The noise function is a measure of the equivalent strain induced by instrument noise. Self gravity noise, residual gas damping and minor fluctuations in the laser amplitude and frequency can simulate strain that could be mistaken for a passing gravitational wave [11]. The response function relates the strain produced by a gravitational wave to the time delay experienced by the beams propagating between pairs of spacecraft in the LISA system. The two functions are combined to form a plot used to determine the signal to noise expected for LISA.

The noise function is dependent only upon instrument parameters and the detector environment. Neither the polarization nor the frequency nor any other aspect of a gravitational wave shows up in the noise function. Consequently, every study of LISA's sensitivity, regardless of the polarization or source direction examined should contain the same noise function. Therefore, the main focus of this study is to develop and analyze the response function of LISA for the scalar polarization predicted in BD.

Systems engineers are often concerned with developing a mathematical formula that relates the input to a system to the expected output. The formula sought is often referred to as a transfer function. A response function is very similar to a transfer function in the way it relates the gravitational wave, which may be considered the input, to the spatial strain experienced by the laser light traveling between two spacecraft. To better understand the response function, consider an analogous situation involving corks floating on a pond.

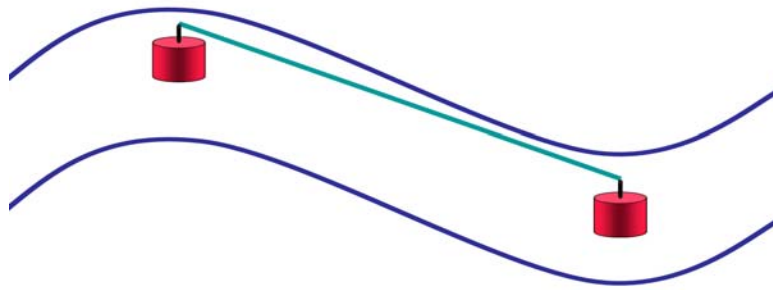


Figure 10: The distance between two corks changes as they bob up and down on waves across a pond. The green line represents a hypothetical rubber band used to measure the changes in distance between the corks.

A lightweight rubber band stretched between the corks stretches as a wave on the pond causes the corks to move up and down. If details of the wave moving the corks are known, i.e. the amplitude, frequency, direction and speed, then it would be possible to generate a mathematical model to calculate how much the rubber band will stretch when disturbed by a passing wave. The response function is the backbone of such a model because it is able to incorporate the effects of different frequencies and source directions of the incident wave. A wave originating from the right or left of the corks depicted in Fig. 10 would produce a response that varies in time. In the case where the waves were originating from above or below the page (Fig.11), both corks could simultaneously be at the crest or the trough of the wave and the rubber band would not stretch at all.

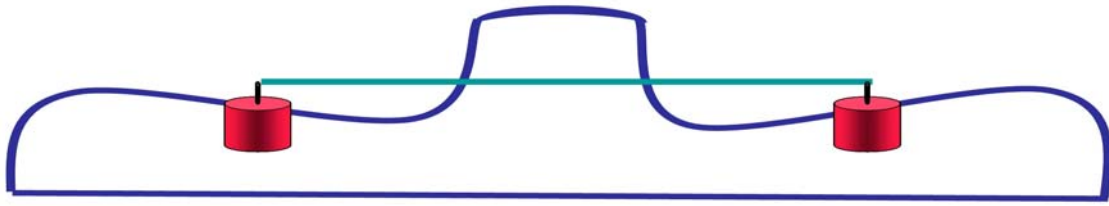


Figure 11: The direction of the incident waves affects how the distance between the corks changes. In this picture, the waves are rolling into the page while both corks are bobbing up and down in unison.

The situation in which the rubber band does not stretch is termed a null response. The frequency of the wave may also produce a null response; in fact, as the frequency of the wave increases, the wavelength will become shorter until it matches the distance between the corks. At that point both corks would reside on different crests and the rubber band would not be stretched (Fig. 12). The response function should indicate a series of null responses as the frequency continues to increase and the distance between the corks becomes equal to integer multiples of the wavelength.

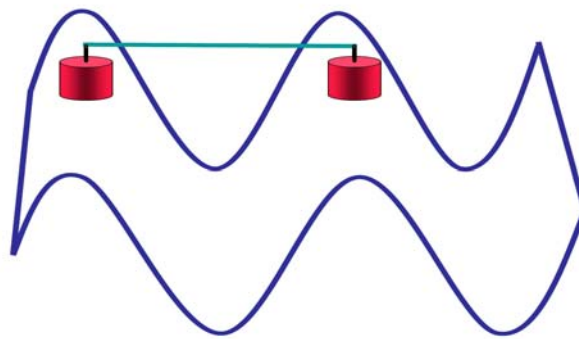


Figure 12: The frequency of incident waves also affects the response function. The distance between corks does not change because the corks float on the same location of different wave crests.

Before an equation can be developed to describe the response function of LISA, the gravitational wave must be described mathematically. A gravitational wave can be approximated as a perturbation of spacetime, so the description of a gravitational wave must begin with the description of spacetime. A relatively small region of space and time can be considered flat to a first order approximation. The spacetime interval for a flat region may be calculated using the metric of special relativity (See Eq. 3) written here in differential form:

$$ds^2 = dx^2 + dy^2 + dz^2 - dt^2, \quad c = 1. \quad (4)$$

The spacetime interval may also be written in metric form;

$$ds^2 = \begin{bmatrix} cdt & dx & dy & dz \end{bmatrix} \begin{bmatrix} -1 & 0 & 0 & 0 \\ 0 & 1 & 0 & 0 \\ 0 & 0 & 1 & 0 \\ 0 & 0 & 0 & 1 \end{bmatrix} \begin{bmatrix} cdt \\ dx \\ dy \\ dz \end{bmatrix}. \quad (5)$$

The flat metric $\begin{bmatrix} -1 & 0 & 0 & 0 \\ 0 & 1 & 0 & 0 \\ 0 & 0 & 1 & 0 \\ 0 & 0 & 0 & 1 \end{bmatrix}$ is symbolized as $\eta_{\mu\nu}$, where μ and ν are indices that range in value from 0

to 3 [8]. Therefore,

$$ds^2 = \sum_{\mu=0}^3 \sum_{\nu=0}^3 \eta_{\mu\nu} dx^\mu dx^\nu. \quad (6)$$

Using Einstein's summation notation, the summations over μ and ν are implied by the repeated indices and no \sum is used;

$$ds^2 = \eta_{\mu\nu} dx^\mu dx^\nu . \quad (7)$$

Equation 7 can then be modified to represent a gravitational wave. For example, the spacetime interval for a perturbation to flat spacetime by a transverse gravitational wave propagating along the z axis is given by

$$ds^2 = (\eta_{\mu\nu} + h_{\mu\nu}) dx^\mu dx^\nu . \quad (8)$$

Here the perturbation matrix is:

$$h_{\mu\nu} = \begin{bmatrix} 0 & 0 & 0 & 0 \\ 0 & h_{xx} & h_{xy} & 0 \\ 0 & h_{yx} & h_{yy} & 0 \\ 0 & 0 & 0 & 0 \end{bmatrix} A \cos(\theta + \delta) \quad (9)$$

For the sake of simplifying the notation, coefficient matrices will be denoted with a capital letter, i.e.

$$h_{\mu\nu} = H_{\mu\nu} A \cos(\theta + \delta) . \quad (10)$$

The amplitude, A , of the perturbation must necessarily be much less than one, which is consistent with predicted strain amplitudes of gravitational waves (on the order of 10^{-21}). In matrix form, the coefficients of the perturbation matrices for the cross, plus, and scalar polarizations in the source frame are given below.

$\begin{bmatrix} 0 & 0 & 0 & 0 \\ 0 & 0 & 1 & 0 \\ 0 & 1 & 0 & 0 \\ 0 & 0 & 0 & 0 \end{bmatrix}$	$\begin{bmatrix} 0 & 0 & 0 & 0 \\ 0 & 1 & 0 & 0 \\ 0 & 0 & -1 & 0 \\ 0 & 0 & 0 & 0 \end{bmatrix}$	$\begin{bmatrix} 0 & 0 & 0 & 0 \\ 0 & 1 & 0 & 0 \\ 0 & 0 & 1 & 0 \\ 0 & 0 & 0 & 0 \end{bmatrix}$
Cross	Plus	Scalar

GR predicts only the cross and plus polarizations, while BD predicts all three. The term ‘source frame’ is in reference to the orientation of the coordinate axes at the source, where the z axis is reserved for the direction of propagation. It is important to note that LISA must be described by a set of coordinate axes that are independent of those in the source frame (See Fig. 13).

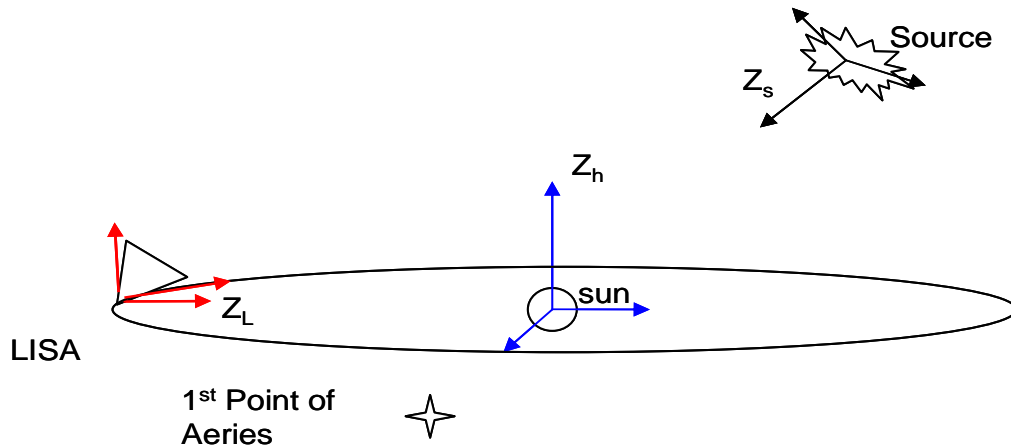


Figure 13: An illustration depicting the relationship between the source, heliocentric, and LISA reference frames. z_s indicates the z axis of the source frame while z_h , and z_L indicate the z axes of the heliocentric and LISA frames respectively.

Ignoring the orbital motion around the sun and assuming LISA remains fixed in space, two rotations are required to transform from the source frame to the LISA frame. An additional three rotations are required when taking the orbital motion of LISA into account [7]. The process of calculating the transformations is outlined in appendix A. It is important to note that the rotations only affect the coefficient matrix.

With the description of the gravitational wave in the LISA coordinate frame, it is possible to investigate how the wave influences the spacetime traveled by the laser beams passing between the spacecraft. The light travels along a null geodesic, which is a path in spacetime where the spacetime interval is equal to zero.

$$0 = (\eta_{\mu\nu} + H_{\mu\nu} A \cos(\omega t - \vec{k} \cdot \vec{r} + \delta)) dx^\mu dx^\nu, \quad \theta = \omega t - \vec{k} \cdot \vec{r}. \quad (11)$$

Here \vec{k} is the vector associated with the propagation direction and wavelength of the gravitational wave, \vec{r} is the vector associated with the distance traveled by the light along an arm of LISA, and δ is a phase constant. Allowing A to equal one will produce a response function that indicates the fraction of the wave's amplitude that is measured by the detector. The light travel time between spacecraft, τ , is approximately 16 seconds. For waves with periods shorter than 16 seconds, the space is alternately stretched and compressed as the light pulse travels between spacecraft. The result is a roll-off in the response for frequencies above 10^{-1} Hz. Separating the time component from the space components yields

$$dt^2 = (\eta_{nm} + H_{nm} A \cos(\omega t - \hat{k} \cdot \hat{r} + \delta)) dx^n dx^m. \quad (12)$$

The subscripts n and m are indices that range from 1 to 3, and include only the spatial components of the matrices. Taking the square root of both sides allows for an integration of the light travel time. Because the perturbations to spacetime are small, the binomial expansion may be employed to rid the integral of the radical.

$$\int_0^{\tau_0} dt = \int_0^{\tau_0} \left(\eta_{nm} + \frac{1}{2} H_{nm} A \cos(\omega t - \hat{k} \cdot \hat{r} + \delta) \right) dx^n dx^m . \quad (13)$$

The integral on the right hand side is evaluated over the spacetime path of a light pulse traveling along the arm of LISA being examined. Note that dx , dy , and dz can be defined in terms of the original length of the arm when the LISA frame is defined (See Fig. 14).

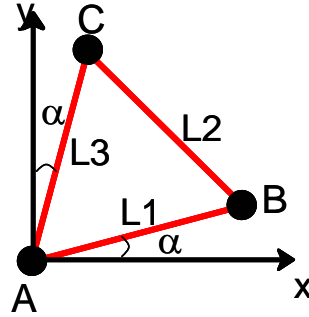


Figure 14: The LISA frame. For an integration along L_1 : $dx = dt \cos(\alpha)$, $dy = dt \sin(\alpha)$, and $dz = 0$.

The response function reflects the time delay for light traveling an arm of LISA and is therefore given by:

$$R(\omega, \tau, \delta) = \frac{\tau' - \tau_0}{\tau_0} =$$

$$\frac{1}{2\tau_0} \int_0^{\tau_0} [H_{11} \cos^2(\alpha) + H_{12} \cos(\alpha) \sin(\alpha) + H_{21} \sin(\alpha) \cos(\alpha) + H_{22} \sin^2(\alpha)] \cos(\omega t - \hat{k} \cdot \hat{r} + \delta) dt. \quad (14)$$

The remaining integral may be solved analytically.

Results

For this study, MATLAB was used to produce two programs to numerically evaluate and compare response functions generated with respect to the three different polarizations predicted by BD. The first program computes the response functions for each polarization and data collection mode by averaging over all incident source directions. The second program calculates the instrument response to gravitational waves originating from the galactic center as LISA orbits the sun.

To validate the mathematics and programming employed to calculate the response functions, the results of the two-arm Michelson to GR polarizations computed by the averaging program were compared to those published by Larson, Hiscock, and Hellings (LHH) in 1999 (See Fig. 15). Minor discrepancies between the plots are the result of different approaches and mathematical approximations. The LHH study involved a complicated approach to calculate the detector response in terms of the power of the gravitational wave, while the approach taken in this study determines the response in terms of the amplitude of the gravitational wave. In addition, the LHH approach assumes a slightly different arm length reflected as a small shift along the $\log(u)$ axis. The logarithmic plot of the power response for this study (illustrated in Figure 15) was generated by taking the log of the square of the amplitude.

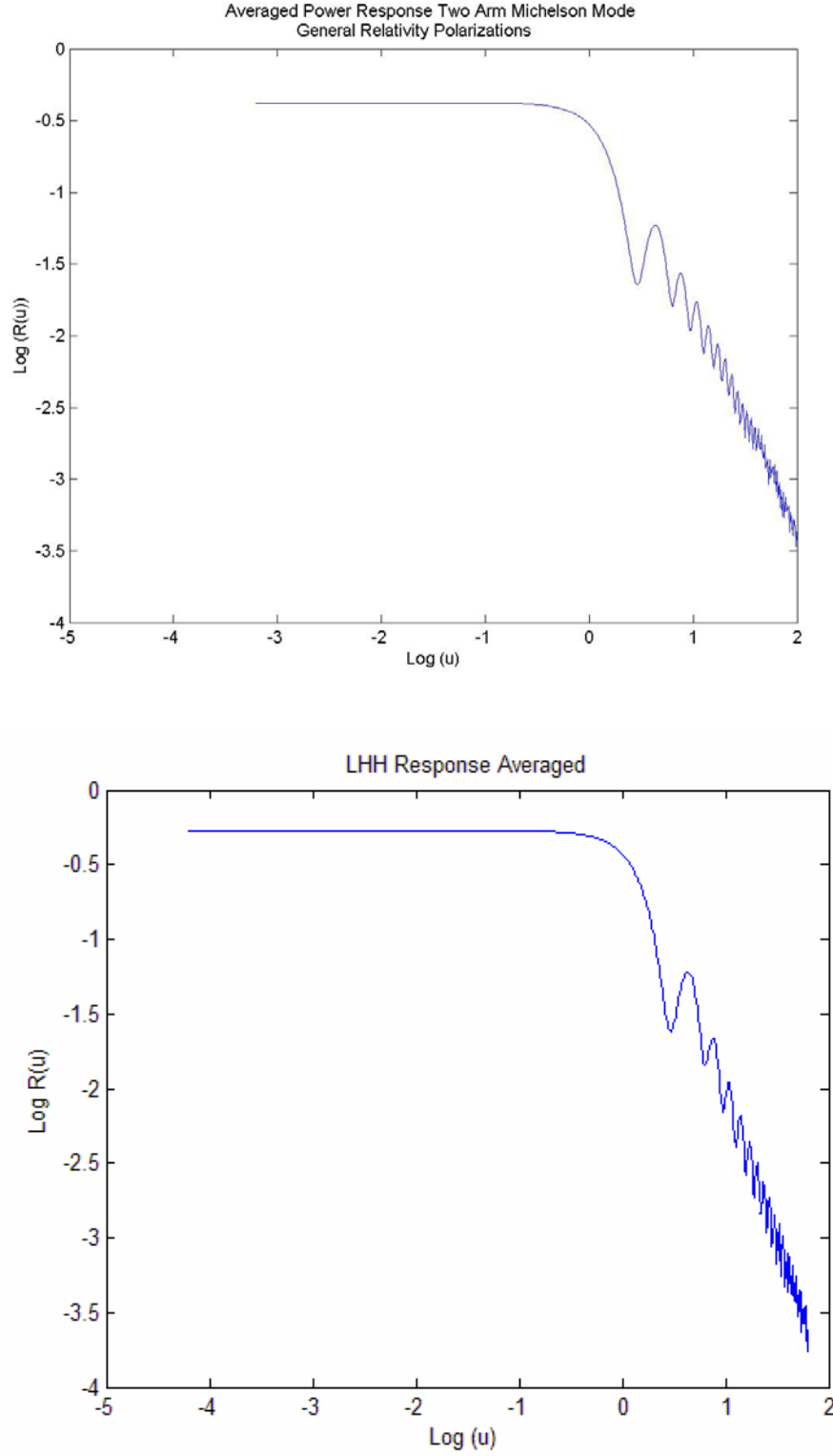


Figure 15: The averaged power response for GR polarizations interacting with LISA in the Two Arm Michelson mode found in this study (top) is compared to the power response of LISA published by Shane Larson, William Hiscock and Ronald Hellings in 1999 (bottom) [11]. The variable u represents the angular frequency ($2\pi f$).

Once it was established that the program could produce reliable results, plots of the averaged LISA response to the scalar polarization were generated for comparison to the averaged LISA response to GR polarizations. The response functions were generated for each mode of data collection, which includes the single arm mode, the two-arm Michelson mode, the three-arm Michelson mode, and the three-arm Sagnac mode. The calculated averaged response functions are presented as Figures 16 - 19.

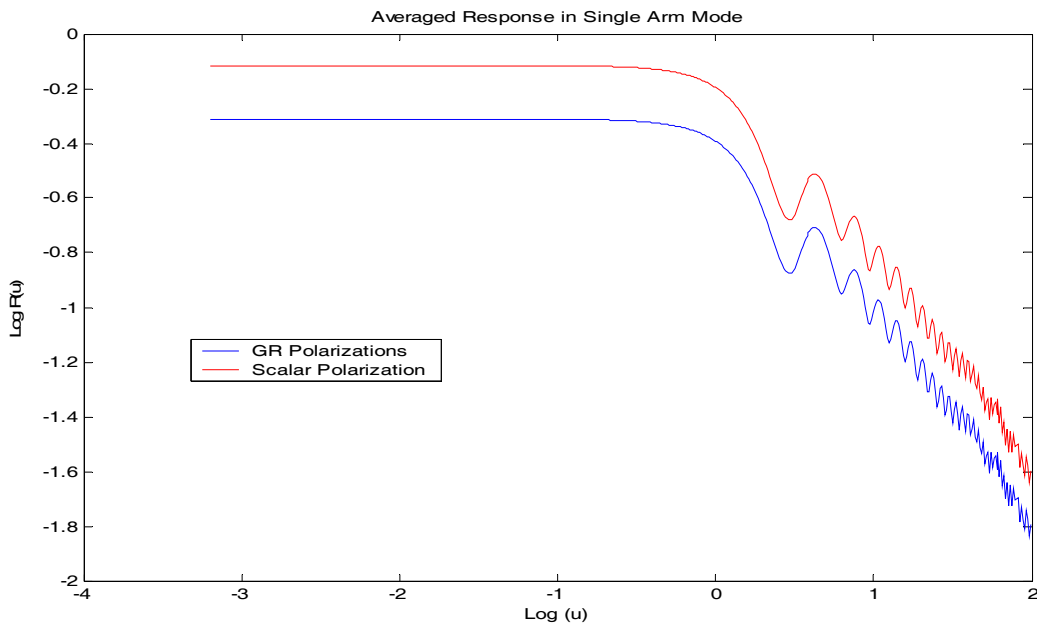


Figure 16: The single arm response.

The comparative response functions are built on the assumption that the amplitude of the scalar polarization is equal to the amplitude of the GR polarizations, although most theories predict a smaller amplitude for the scalar wave. Figure 16 indicates the averaged scalar response is stronger than the averaged GR response in the single arm mode. The stronger scalar response is a direct result of the symmetry of the scalar polarization, which results in fewer null responses associated with the source direction of the gravitation wave.

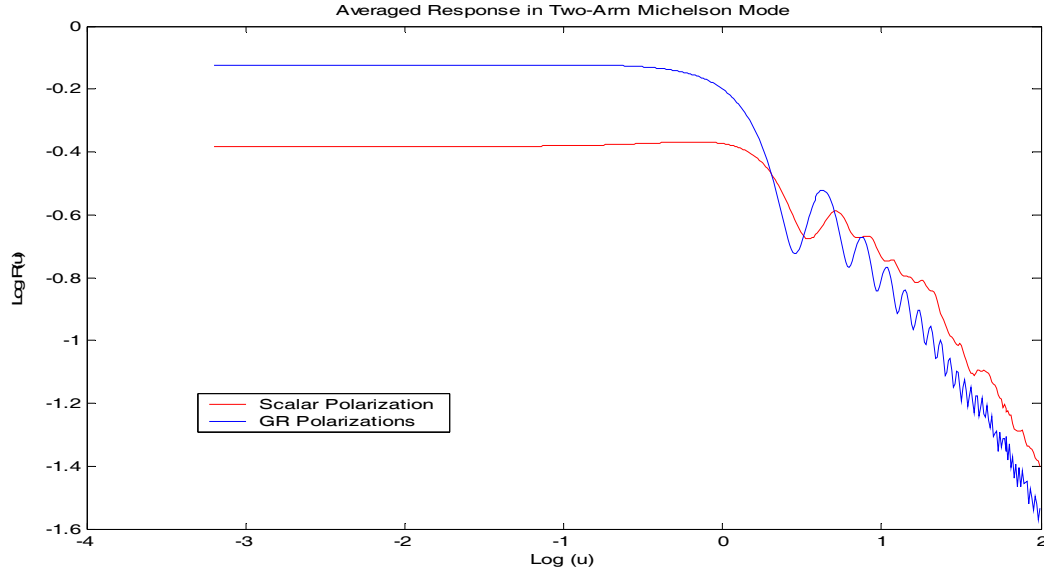


Figure 17: The two-arm Michelson response.

The two-arm Michelson mode enhances the response to GR polarizations for low frequencies while suppressing the scalar response. The results are intuitively clear considering GR polarizations act to stretch one arm while shrinking the second causing a greater difference in arm-lengths. The scalar polarization in low frequencies acts to stretch or shrink both arms simultaneously, thereby minimizing the difference in arm-lengths. A similar argument can be posed for the three-arm Michelson mode (See Fig. 18). However, it is also important to note that at high-frequencies for which the wavelengths of gravitational waves are shorter than the arm length of the detector, the periodic cancellations that reduce the response to the GR polarizations provide a relative enhancement for the response to the scalar polarization. As the program calculates the response function it assumes an initial phase of the gravitational wave at the detector. Because the phase of the gravitational wave producing the maximum response is unknown, the program increments this phase, finding and storing the maximum, which is the amplitude of the sinusoidal response.

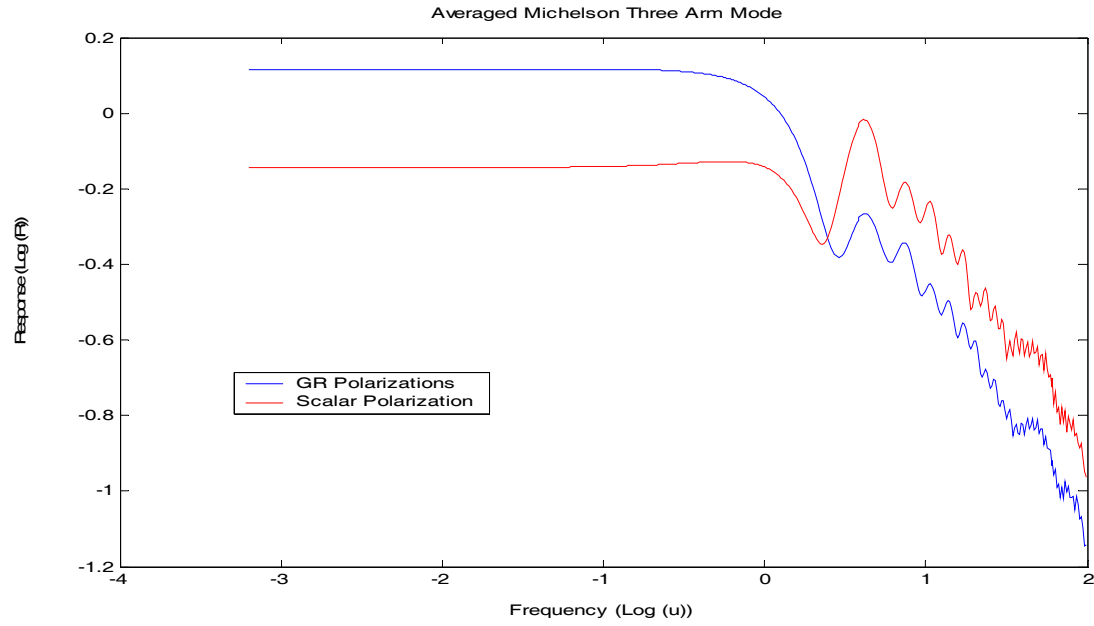


Figure 18: The three-arm Michelson response..

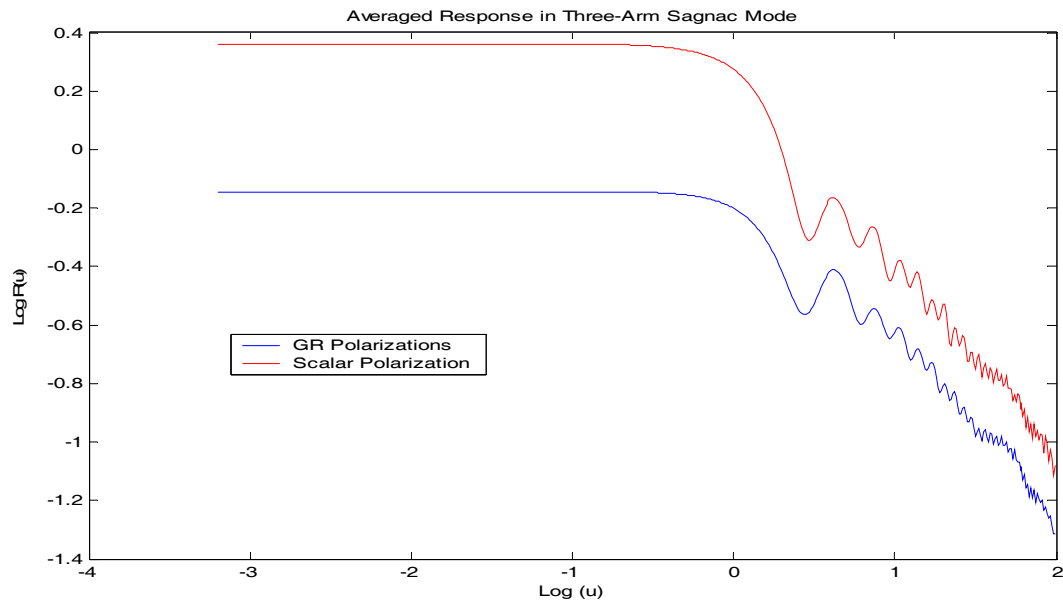


Figure 19: The three-arm Sagnac response.

The three-arm Sagnac mode provides the greatest response to the scalar polarization. Though the response function suggests the three-arm Sagnac mode is the most likely to detect a scalar gravitational wave, a complete sensitivity analysis of LISA requires an examination of the noise in the three-arm Sagnac mode, which may be significantly greater than the noise in the Michelson modes.

The LISA response to gravitational waves from a particular direction in the sky will vary as the detector orbits the sun. In order to examine the response of LISA to gravitational waves of various frequencies and polarizations originating from the center of the galaxy, a three dimensional plot was generated for each mode of data collection. For each three dimensional plot, the abscissa was chosen to indicate orbital position ranging from 0 to 360 degrees. The ordinate indicates the log of the angular frequency of the incident gravitational wave ($\log(f)$, where f is measured in Hz); and the log of the magnitude of the response is plotted on the z axis. The comparative plots for each mode of data collection are presented as Figures 20 - 24.

Figure 20 displays the single arm response for each arm of LISA to GR gravitational waves originating from the direction of the galactic center. The fluctuations in the response throughout the orbit depend heavily upon the initial orientation of each arm. L_1 exhibits a fairly uniform response across the orbital, so it was chosen for a comparison with the single-arm mode response to scalar gravitational waves (See Fig. 21).

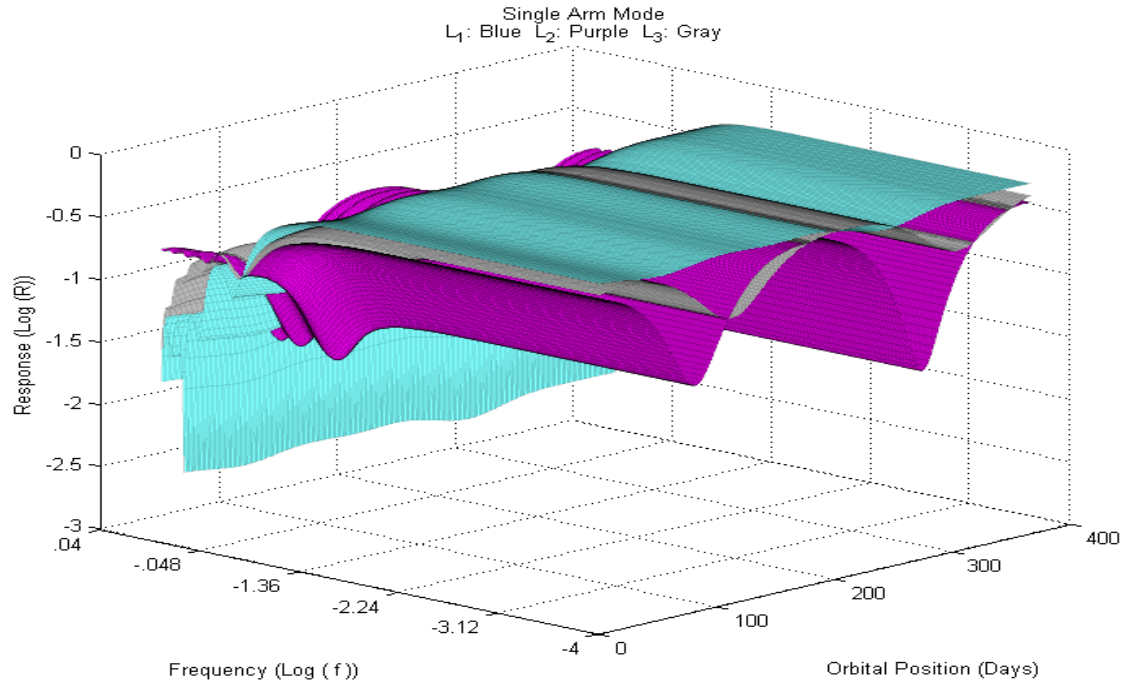


Figure 20: Single arm response functions for averaged GR polarizations propagating from the galactic center.

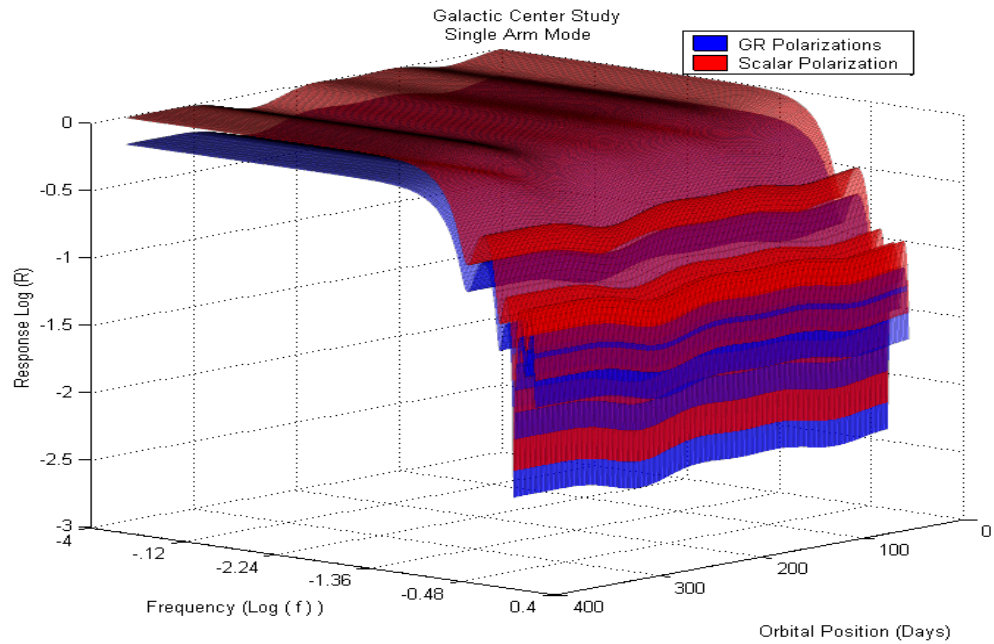


Figure 21: Single arm response functions for the scalar and averaged GR polarizations propagating from the galactic center.

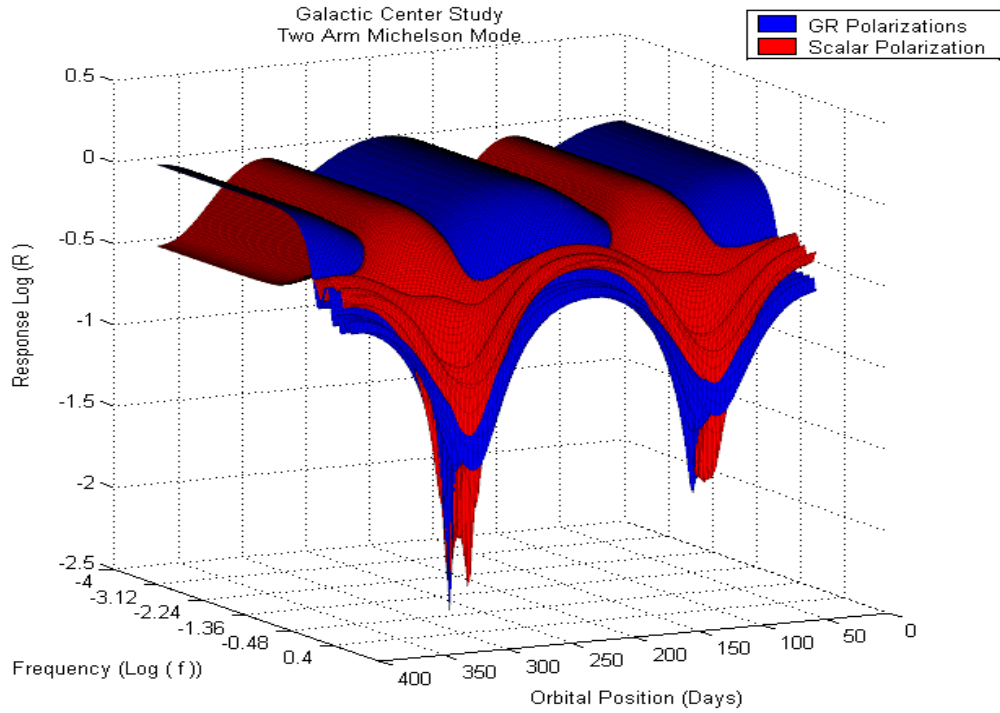


Figure 22: The two-arm Michelson response functions for the scalar and averaged GR polarizations propagating from the galactic center.

The response functions plotted for the two-arm Michelson mode (See Fig. 22) indicate that the maximum responses to low-frequency scalar gravitational waves will occur at orbital positions that differ from those exhibiting the maximum responses to GR polarizations. The separation of maximum-response locations provides a distinguishing feature when the source location is known.

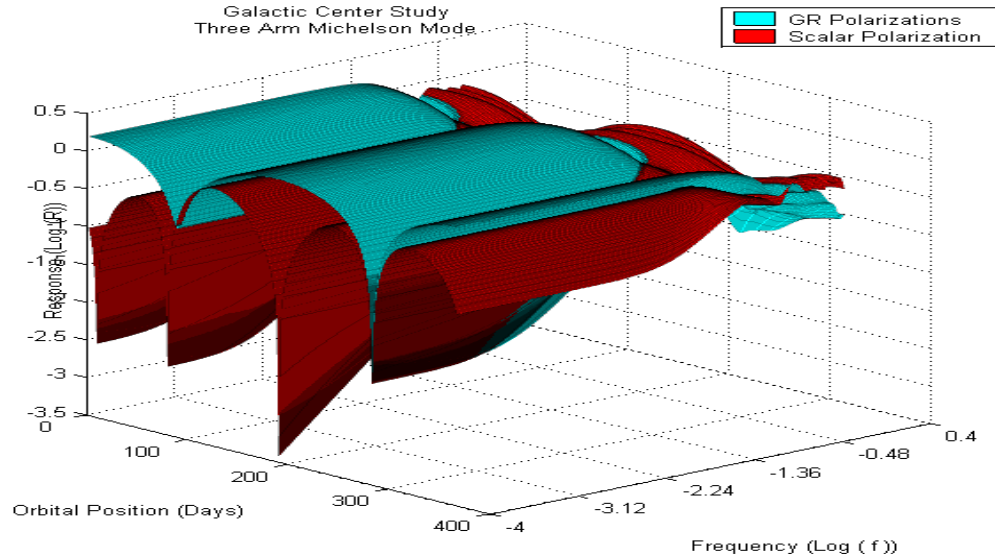


Figure 23: The three-arm Michelson response functions for the scalar and averaged GR polarizations propagating from the galactic center.

The sharp dips in the LISA response to scalar waves measured in the three-arm Michelson mode provide an essential distinguishing feature between the scalar and GR polarizations (See Fig. 23). A dramatic drop in signal strength at four locations in LISA's orbit would indicate the presence of a scalar polarized gravitational wave. Moreover, the location of signal losses provides information about the source direction. Comparing signal response fluctuations in the two-arm Michelson mode with those measured in the three-arm Michelson mode will provide greater precision in the determination of polarization and source direction.

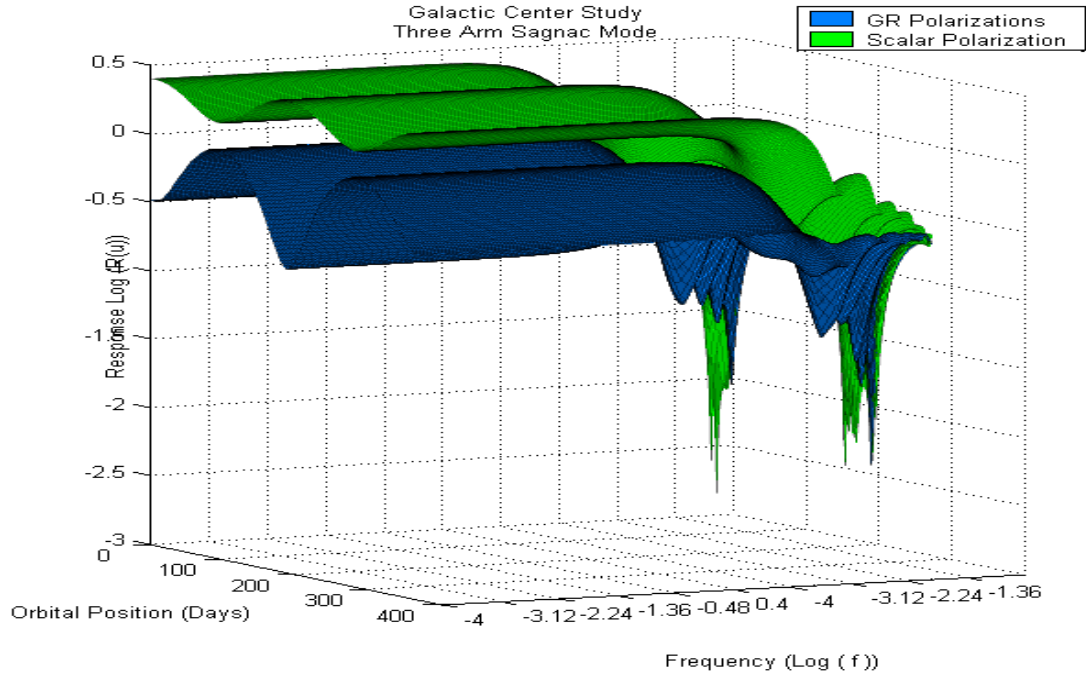


Figure 24: The three-arm Sagnac response functions for the scalar and averaged GR polarizations propagating from the galactic center.

The orbital variations in response displayed in the three-arm Sagnac mode are similar to those produced in the two-arm Michelson mode; however, the scalar response exhibits a significant enhancement in magnitude. The Sagnac mode provides improved scalar response because the lengths of the arms are summed rather than subtracted from one another.

To examine the LISA response to gravitational waves of a particular frequency originating from the direction of the galactic center, data from the low frequency end of the three dimensional plots were converted to polar form. The magnitude of the response was scaled by a factor of 100 before its logarithm was computed so that the logarithm would be positive and then plotted as the radial coordinate of a polar plot. The angular coordinate in the polar plots corresponds to the orbital position of LISA in the heliocentric frame. Two polar graphs were created to display the response functions for GR polarizations and the scalar polarization for each mode of data collection. This representation of the response as a function of orbital position

provides characteristic patterns that distinguish each polarization and mode combination. The plots are presented as Figures 25 and 26.

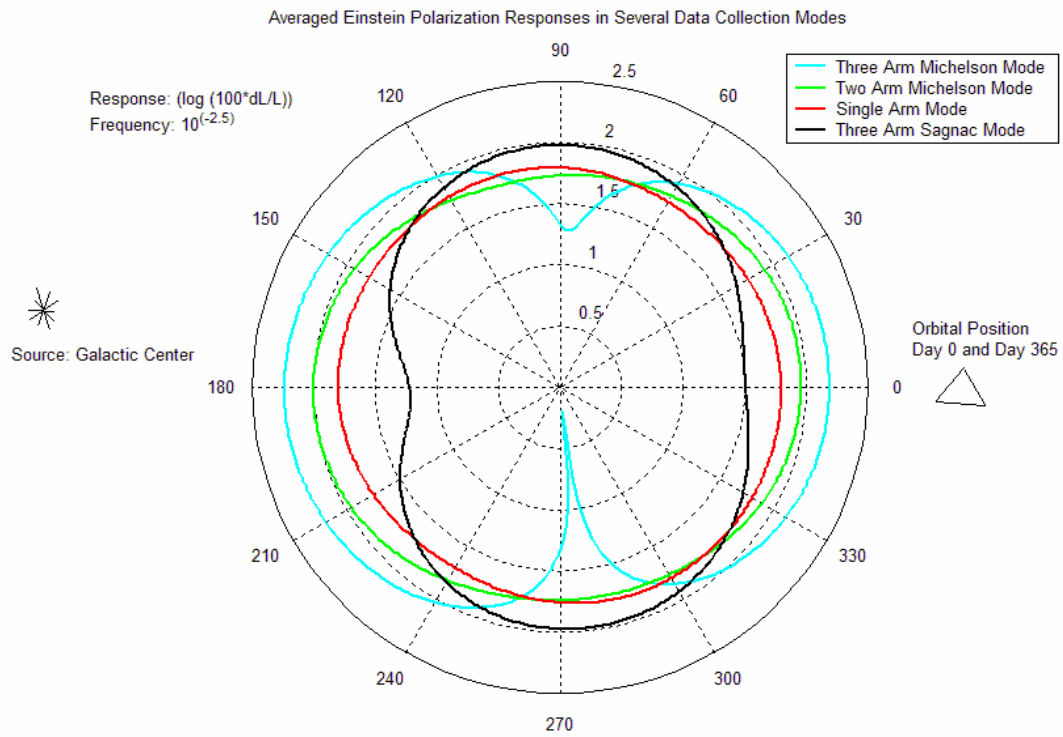


Figure 25: The response functions calculated with respect to the polarizations predicted by GR for four different modes of data collection.

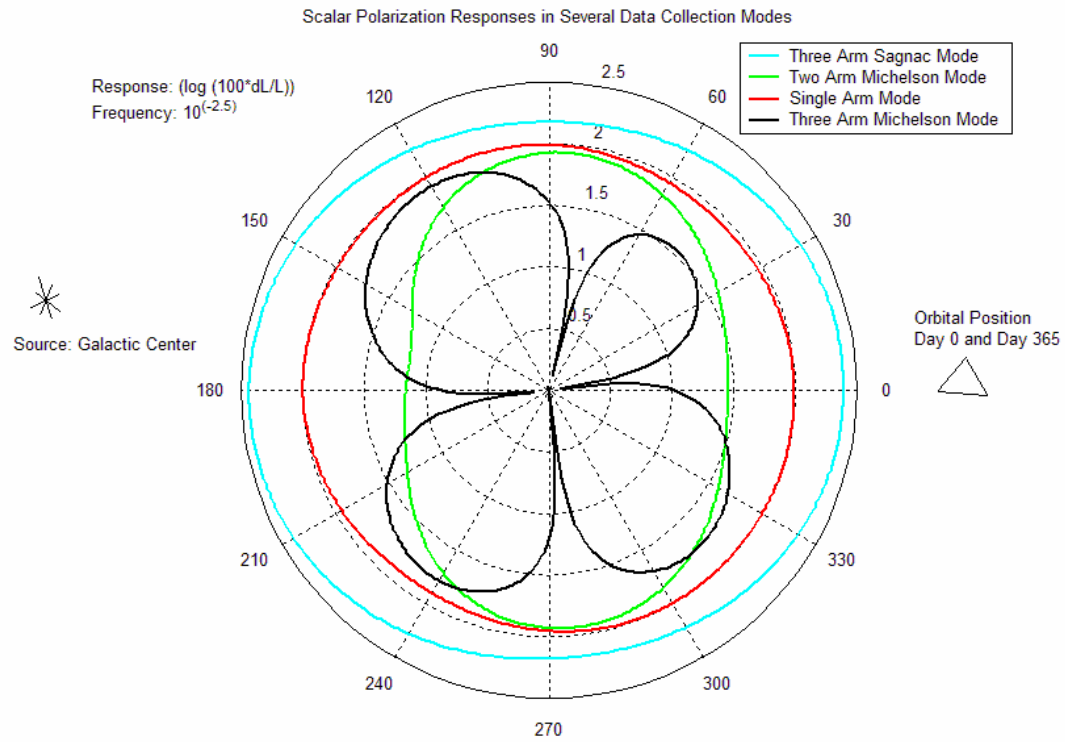


Figure 26: The response functions calculated with respect to the scalar polarization for four different modes of data collection.

It is important to note that the response functions were generated assuming that the three arms of LISA are of equal length and the original distance between pairs of spacecraft is very precisely known. The study published by LHH presents the argument that assuming the arms are of equal and known length will lead to response functions that are accurate first order representations of the actual unequal arm design of the LISA detector. The approximation is appropriate for this study, as it is mainly concerned with comparing the LISA response functions generated with respect to the GR and scalar polarizations.

Conclusions

The primary goal of this study was to determine if a gravitational wave of scalar polarization with sufficient amplitude could be detected and distinguished from the plus and cross polarizations. The results of the study indicate that LISA will be able to detect and identify the scalar polarization provided the amplitude of gravitational waves exhibiting the scalar polarization is comparable to the amplitude of gravitational waves exhibiting GR polarizations. Additionally, the results show that a comparison of the variations in responses measured by several data collection modes will indicate the direction of the source. When LISA becomes operational, variances in the strength of a detected signal may be compared to signature features of the response functions, such as the number of dips and their relative sharpness, in order to determine the propagation direction and polarization of the measured gravitational wave. These results will provide input for future researchers to determine the optimal data collection method to detect gravitational waves of a given polarization, frequency, and source direction and may also be used to develop algorithms to identify the polarizations and directionality of gravitational waves from data transmitted from the detector.

Appendix A

A major task in developing the response function was to describe the gravitational wave in the LISA frame. The challenge in determining the description of the gravitational wave in the LISA frame resides in the fact that LISA's orientation relative to the source changes as it orbits the sun. Several orbital parameters outlined in the Pre-phase A Report [7] developed by NASA made it possible to include the orbital dynamics in the mathematical model constructed within this study. The following parameters were included in the model.

First, the plane formed by the three spacecraft forms a 60 degree angle with the x-y plane of the heliocentric frame (See Fig. A1). Secondly, the equilateral triangle formed by the spacecraft rotates 360 degrees clockwise about the z axis of the LISA frame as it follows earth in one revolution about the sun (See Fig. A1).

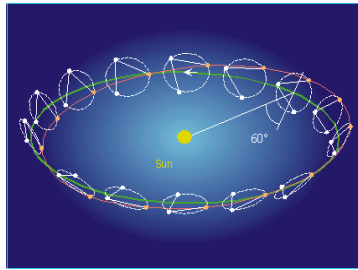


Figure A1: An illustration of the 60 degree inclination to the plane of the ecliptic, and the clockwise rotation of LISA over the period of the orbit [10].

Third, the orbital position of LISA has been divided into days, with day zero arbitrarily chosen such that the x axis of the LISA frame parallels the x axis of the heliocentric frame. The x axis of the heliocentric frame points from the sun to the First Point of Aries.

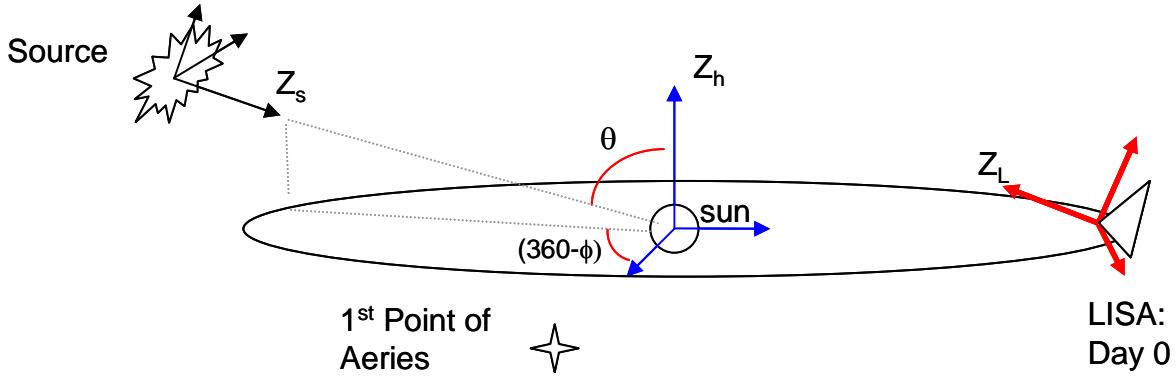


Figure A2: The LISA frame at its starting point in its orbit about the sun.

Five rotations are used to transform from the descriptions of the gravitational wave in the source frame to the description of the gravitational wave in the LISA frame. Each rotation is described in terms of the polar angles θ and ϕ defined in the heliocentric frame (See Fig. A2). The first two rotations bring the source frame into the heliocentric frame, while the last three rotations transform between the heliocentric frame and the LISA frame.

The y axis of the source frame is assumed to be coplanar with the z axis of the heliocentric frame. (Note: Any adverse implications of this assumption are nullified by averaging the response over the plus and cross polarizations; and the assumption has no effect on the calculation of the response with respect to the scalar polarization due to the symmetric properties of the strain pattern.) The rotations are listed in order in Table A1.

Rotation	Axis of Rotation	Angle Subtended
R_1	X	$\pi-\theta$
R_2	Z	$\pi/2-\phi$
R_3	Z	$2\pi t/365$
R_4	X	$\pi/3$
R_5	Z	$-2\pi t/365$

R_1	X	$\pi-\theta$
R_2	Z	$\pi/2-\phi$
R_3	Z	$2\pi t/365$
R_4	X	$\pi/3$
R_5	Z	$-2\pi t/365$

Table A1: The first two rotations listed are used to convert the source frame into the heliocentric frame. The remaining three rotations convert to the LISA frame. Here the variable t represents the number of days elapsed in LISA's orbit about the sun.

Rotations about the x and z axes are provided by the following equations.

$$R_x = \begin{bmatrix} 1 & 0 & 0 \\ 0 & \cos(\psi) & \sin(\psi) \\ 0 & -\sin(\psi) & \cos(\psi) \end{bmatrix} \quad (A1)$$

$$R_z = \begin{bmatrix} \cos(\psi) & \sin(\psi) & 0 \\ -\sin(\psi) & \cos(\psi) & 0 \\ 0 & 0 & 1 \end{bmatrix} \quad (A2)$$

Here ψ is the angle subtended in the rotation. By convention, the wave propagates in the Z direction of the source frame. So the propagation direction of the gravitational wave in the LISA frame (κ_{LISA}), is given by equation A3.

$$\kappa_{LISA} = R_5 R_4 R_3 R_2 R_1 \begin{bmatrix} 0 \\ 0 \\ 1 \end{bmatrix} \quad (A3)$$

The metric describing the gravitational wave represents a tensor, so the original matrix must also be multiplied by the transpose of each rotation.

$$H_{\mu\nu_{LISA}} = \{R_5 R_4 R_3 R_2 R_1 [H_{\mu\nu_{source}}] R_1^t R_2^t R_3^t R_4^t R_5^t\} \quad (A4)$$

The perturbation matrix in the LISA frame is therefore written as:

$$h_{\mu\nu_{LISA}} = \{R_5 R_4 R_3 R_2 R_1 [H_{\mu\nu_{source}}] R_1^t R_2^t R_3^t R_4^t R_5^t\} A \cos(\theta + \delta) \quad (A5)$$

These rotations are construction on the assumption that the initial orbital position of LISA is on the y-axis of the heliocentric frame.

Appendix B

The following MATLAB® code calculates the response functions averaged over all possible source directions.

```
function Z = AverageAllSky ()
% Function that will determine the LISA response for plus, cross, and
% scalar polarizations in an all sky average. The program also allows for a
% linear combination of cross and plus, and a linear combination of cross
% and scalar polarizations.

% Begin clock to measure the program run-time.
tic

% The perturbation matrices
hcross = [0 1 0; 1 0 0; 0 0 0];
hplus = [1 0 0; 0 -1 0; 0 0 0];
hscalar = [1 0 0; 0 1 0; 0 0 0];

% The Mixfactor is the coefficient in a linear combination of cross and
% scalar polarizations. For example: Mixfactor = .1 would mean that the
% matrix element of the calculations consists of hx + .1*hs, where hx is
% the matrix element for the cross polarization and hs is the matrix
% element for the scalar polarization.
Mixfactor = .1;

% tstep gives the sample size in days. For example: tstep =1 then the
% response will be calculated for each day of its orbit.
tstep = 10;
tdays = [0:tstep:365];

% The range of frequencies
uu = 2*pi*(10.^(-4:.01:1.2));

% Matricies used to store values
[r,c] = size (uu);
[rr,cc] = size (tdays);

A = ones(c,cc);
B = A;
C = A;
D = A;
E = A;
F = A;

ScalarA = A;
ScalarB = A;
ScalarC = A;
ScalarD = A;
ScalarE = A;
ScalarF = A;

ComboA = A;
ComboB = A;
ComboC = A;
ComboD = A;
ComboE = A;
ComboF = A;

% The values associated with alpha in the LISA frame and store in
```

```

% memory for later use. Alpha is the angle between an arm of LISA and the
% x-axis of the LISA frame.
csal=cos(pi/12);
csalS=csal^2;
csa2=cos(5*pi/12);
csa2S=csa2^2;
csa3=cos(3*pi/4);
csa3S=csa3^2;
snal=sin(pi/12);
snalS=snal^2;
sna2=sin(5*pi/12);
sna2S=sna2^2;
sna3=sin(3*pi/4);
sna3S=sna3^2;

% Counting numbers used to designate where data is stored.
n=0;
N=0;
nn=0;

% The ranges and step sizes for theta, phi, and epsilon.
theta1 = [pi/16:(pi/8):(11*pi/16)];
[rtheta, ctheta] = size (theta1);

phil = [pi/16:(pi/8):(31*pi/16)];
[rphi, cphi] = size (phil);

epsilonstep = 1/16;
epsilon1 = [(pi*epsilonstep)/2):(pi*epsilonstep):((2/epsilonstep)-1)*pi...
            *(epsilonstep/2)];
[reps,ceps] = size (epsilon1);

% The final rotation that orients the LISA frame sixty degrees
% relative to the plane of the ecliptic.
RorbitTilt = [1 0 0; 0 cos(pi/3) sin(pi/3); 0 -sin(pi/3) cos(pi/3)];

% A series of nested loops numerically evaluates the response function.
for theta = theta1

    % The values associated with theta including the first rotation
    % required to translate between the source frame and the heliocentric frame.
    cth= cos(theta);
    sth= sin(theta);
    RTheta = [1 0 0; 0 cos(pi-theta) sin(pi-theta); 0 -sin(pi-theta)...
              cos(pi-theta)];

    for phi = phil

        % Each value of nn corresponds to a unique source location.
        nn= nn+1;

        % The values used in the calculation of the
        % response function that include the variable phi.
        muone= -sth*cos(phi-pi/12);
        mutwo= -sth*cos(phi-5*pi/12);
        muthree= -sth*cos(phi-3*pi/4);

        % The second rotation required to translate between the
        % source and heliocentric frame.
        RPhi = [cos(pi/2-phi) sin(pi/2-phi) 0; -sin(pi/2-phi) cos(pi/2-phi)...
                0; 0 0 1];

```

```

% The perturbation matrices in the heliocentric frame.
hHcross = RPhi'*RTheta'*hcross*RTheta*RPhi;
hHplus = RPhi'*RTheta'*hplus*RTheta*RPhi;
hHscalar = RPhi'*RTheta'*hscalar*RTheta*RPhi;

% Clear the matrices used to temporarily store the response function
% calculated for a particular value of theta and phi.
A = zeros(c,cc);
B = A;
C = A;
D = A;
E = A;
F = A;

ScalarA = A;
ScalarB = A;
ScalarC = A;
ScalarD = A;
ScalarE = A;
ScalarF = A;

ComboA = A;
ComboB = A;
ComboC = A;
ComboD = A;
ComboE = A;
ComboF = A;

% Reset counting variable used to indicate frequency.
N=0;

for u = uu

    % N and n are counting numbers that control the storage of
    % values in Matrices A, B, and C. N corresponds to the
    % frequency and n corresponds to the orbital position.
    N = N + 1;
    n=0;

    for t = tdays

        n=n+1;

        % Rotation matrices that account for LISA's orbit about
        % the sun.
        RphiLISA = [cos((t*2*pi)/365) sin((t*2*pi)/365) 0;...
                    -sin((t*2*pi)/365) cos((t*2*pi)/365) 0; 0 0 1];
        RbackRotate = [cos(-(t*2*pi)/365) sin(-(t*2*pi)/365) 0;...
                       -sin(-(t*2*pi)/365) cos(-(t*2*pi)/365) 0; 0 0 1];

        % The perturbation matrices described in the
        % LISA frame. Three Euler angles are used to transform
        % the perturbation matrices described in the
        % heliocentric frame to those described in the LISA
        % frame.
        hLcross = RbackRotate*RorbitTilt*RphiLISA*hHcross*RphiLISA'...
                  *RorbitTilt'*RbackRotate';
        hLplus = RbackRotate*RorbitTilt*RphiLISA*hHplus*RphiLISA'...
                 *RorbitTilt'*RbackRotate';
        hLscalar= RbackRotate*RorbitTilt*RphiLISA*hHscalar*RphiLISA'...
                  *RorbitTilt'*RbackRotate';

```

```

% The time independent components associated with each
% response function evaluated.
CrossMet1= .5*((hLcross(1,1)*csa1S) + (hLcross(1,2)*csa1*sna1)...
+ (hLcross(2,1)*sna1*csa1) + (hLcross(2,2)*sna1S));
CrossMet2= .5*((hLcross(1,1)*csa2S) + (hLcross(1,2)*csa2*sna2)...
+ (hLcross(2,1)*sna2*csa2) + (hLcross(2,2)*sna2S));
CrossMet3= .5*((hLcross(1,1)*csa3S) + (hLcross(1,2)*csa3*sna3)...
+ (hLcross(2,1)*sna3*csa3) + (hLcross(2,2)*sna3S));

PlusMet1= .5*((hLplus(1,1)*csa1S) + (hLplus(1,2)*csa1*sna1)...
+ (hLplus(2,1)*sna1*csa1) + (hLplus(2,2)*sna1S));
PlusMet2= .5*((hLplus(1,1)*csa2S) + (hLplus(1,2)*csa2*sna2)...
+ (hLplus(2,1)*sna2*csa2) + (hLplus(2,2)*sna2S));
PlusMet3= .5*((hLplus(1,1)*csa3S) + (hLplus(1,2)*csa3*sna3)...
+ (hLplus(2,1)*sna3*csa3) + (hLplus(2,2)*sna3S));

ScalarMet1= .5*((hLscalar(1,1)*csa1S) + (hLscalar(1,2)*csa1...
*sna1) + (hLscalar(2,1)*sna1*csa1) + (hLscalar(2,2)*sna1S));
ScalarMet2= .5*((hLscalar(1,1)*csa2S) + (hLscalar(1,2)...
*csa2*sna2) + (hLscalar(2,1)*sna2*csa2)+(hLscalar(2,2)...
*sna2S));
ScalarMet3= .5*((hLscalar(1,1)*csa3S) + (hLscalar(1,2)*csa3...
*sna3) + (hLscalar(2,1)*sna3*csa3) + (hLscalar(2,2)*sna3S));

% Resetting variables used in calculating the response
% function to zero for the next iteration.
DX1sum=0;
DX2sum=0;
DX3sum=0;
DX12sum=0;
DX123Msum=0;
DX123Ssum=0;

DXScalar1sum=0;
DXScalar2sum=0;
DXScalar3sum=0;
DXScalar12sum=0;
DXScalarM123sum=0;
DXScalarS123sum=0;

DXCombo1sum=0;
DXCombo2sum=0;
DXCombo3sum=0;
DXCombo12sum=0;
DXComboM123sum=0;
DXComboS123sum=0;

% Averaging over epsilon accounts for rotation about
% the third Euler angle required in transforming from
% the source frame to the heliocentric frame.
for epsilon = epsilon1

    % This combination of the plus and cross metric
    % components accounts for the third rotation
    % mentioned in the comment on line 211 (directly
    % above epsilon for loop).
    metepsone = cos(2*epsilon)*CrossMet1 - sin(2*epsilon)...
    *PlusMet1;
    metepstwo = cos(2*epsilon)*CrossMet2 - sin(2*epsilon)...
    *PlusMet2;
    metepsthree = cos(2*epsilon)*CrossMet3 - sin(2*epsilon)...
    *PlusMet3;

```

```

% Combines the scalar polarization with the mixture
% of GR plus and cross polarizations.
ComboCrossScalar1 = metepsone + Mixfactor*ScalarMet1;
ComboCrossScalar2 = metepstwo + Mixfactor*ScalarMet2;
ComboCrossScalar3 = metepsthree + Mixfactor*ScalarMet3;

% Resetting values used in delta loop.
DX1=0;
DX2=0;
DX3=0;
DX12=0;
DX123M=0;
DX123S=0;

DXScalar1=0;
DXScalar2=0;
DXScalar3=0;
DXScalar12=0;
DXScalarM123=0;
DXScalarS123=0;

DXCombo1=0;
DXCombo2=0;
DXCombo3=0;
DXCombo12=0;
DXComboM123=0;
DXComboS123=0;

% Delta is the phase constant for the incident
% wave. (kx-wt+delta) This portion of the program
% finds the amplitude of the response. The
% response will vary depending upon the initial
% phase of the gravitational wave. As the program
% cycles through possible values for the initial
% phase, it stores the maximum response.
for delta = pi/32:pi/16:31*pi/32;

    % f1, f2, and f3 include the time dependent parts for
    % the response function.

    f1= ((sin(delta-muone*u)-sin(delta-u))/(u*(1-muone))...
          +(sin(u+delta)-sin(delta-muone*u))/(u*(1+muone)));
    f2= ((sin(delta-mutwo*u)-sin(delta-u))/(u*(1-mutwo))...
          +(sin(u+delta)-sin(delta-mutwo*u))/(u*(1+mutwo)));
    f3= ((sin(u*(1+muone)-delta)-sin(mutwo*u-delta))...
          /(u*(1-muthree)))+(sin(u*(1-muone)+delta)...
          +sin(mutwo*u-delta))/(u*(1+muthree)));

    % deltaX values correspond to the change in length of
    % each arm. This combines the time independent
    % components with the time dependent component to
    % achieve the complete response of LISA to the
    % gravitational wave. X1 corresponds to L1, X2 to L2,
    % and so on. Similar calculations were computed for
    % the scalar response and the response to the
    % combination of scalar and GR polarizations.
    deltaX1= metepsone*f1;
    deltaX2= metepstwo*f2;
    deltaX3= metepsthree*f3;

    % In order to calculate the response we must find the
    % value of delta that yields the maximum result
    % (indicating amplitude of response).
    if abs(deltaX1) > DX1

```



```

        DX1 = abs(deltaX1);
    end
    if abs(deltaX2) > DX2
        DX2 = abs(deltaX2);
    end
    if abs(deltaX3) > DX3
        DX3 = abs(deltaX3);
    end
    if abs(deltaX1-deltaX2) > DX12
        DX12 = abs(deltaX1-deltaX2);
    end
    if abs(deltaX1+deltaX2-2*deltaX3) > DX123M
        DX123M = abs(deltaX1+deltaX2-2*deltaX3);
    end
    if abs(deltaX1+deltaX2+deltaX3) > DX123S
        DX123S = abs(deltaX1+deltaX2+deltaX3);
    end

    deltaXScalar1 = ScalarMet1*f1;
    deltaXScalar2 = ScalarMet2*f2;
    deltaXScalar3 = ScalarMet3*f3;

    if abs(deltaXScalar1) > DXScalar1

        DXScalar1 = abs(deltaXScalar1);
    end
    if abs(deltaXScalar2) > DXScalar2
        DXScalar2 = abs(deltaXScalar2);
    end
    if abs(deltaXScalar3) > DXScalar3
        DXScalar3 = abs(deltaXScalar3);
    end
    if abs(deltaXScalar1-deltaXScalar2)> DXScalar12
        DXScalar12 = abs(deltaXScalar1-deltaXScalar2);
    end
    if abs (deltaXScalar1+deltaXScalar2-2*deltaXScalar3)...
        > DXScalarM123
        DXScalarM123 = abs (deltaXScalar1+deltaXScalar2...
            -2*deltaXScalar3);
    end
    if abs (deltaXScalar1+deltaXScalar2+deltaXScalar3)...
        > DXScalarS123
        DXScalarS123 = abs (deltaXScalar1+deltaXScalar2...
            +deltaXScalar3);
    end

    deltaXCombo1 = ComboCrossScalar1*f1;
    deltaXCombo2 = ComboCrossScalar2*f2;
    deltaXCombo3 = ComboCrossScalar3*f3;

    if abs(deltaXCombo1) > DXCombo1
        DXCombo1 = abs(deltaXCombo1);
    end
    if abs(deltaXCombo2) > DXCombo2
        DXCombo2 = abs(deltaXCombo2);
    end
    if abs(deltaXCombo3) > DXCombo3
        DXCombo3 = abs(deltaXCombo3);
    end
    if abs(deltaXCombo1-deltaXCombo2)> DXCombo12
        DXCombo12 = abs(deltaXCombo1-deltaXCombo2);
    end
    if abs (deltaXCombo1+deltaXCombo2-2*deltaXCombo3)...

```

```

        > DXComboM123
        DXComboM123 = abs (deltaXCombo1+deltaXCombo2...
        -2*deltaXCombo3);
    end
    if abs (deltaXCombo1+deltaXCombo2+deltaXCombo3)...
        > DXComboS123
        DXComboS123 = abs (deltaXCombo1+deltaXCombo2+...
        deltaXCombo3);
    end

end % End delta loop.

% Add the response functions for each arm and
% each combination of arms.
DX12sum = DX12sum + abs(DX12);
DX1sum = DX1sum + abs(DX1);
DX2sum = DX2sum + abs(DX2);
DX3sum = DX3sum + abs(DX3);
DX123Msum = DX123Msum + abs(DX123M);
DX123Ssum = DX123Ssum + abs(DX123S);

DXScalar1sum=DXScalar1sum + abs(DXScalar1);
DXScalar2sum=DXScalar2sum + abs(DXScalar2);
DXScalar3sum=DXScalar3sum + abs(DXScalar3);
DXScalar12sum=DXScalar12sum + DXScalar12;
DXScalarM123sum=DXScalarM123sum + DXScalarM123;
DXScalarS123sum=DXScalarS123sum + DXScalarS123;

DXCombo1sum=DXCombo1sum + abs(DXCombo1);
DXCombo2sum=DXCombo2sum + abs(DXCombo2);
DXCombo3sum=DXCombo3sum + abs(DXCombo3);
DXCombo12sum=DXCombo12sum + DXCombo12;
DXComboM123sum=DXComboM123sum + DXComboM123;
DXComboS123sum=DXComboS123sum + DXComboS123;

end % End epsilon loop

% Stores the sum of the responses for each angle sampled.
A(N,n) = DX1sum;
B(N,n) = DX2sum;
C(N,n) = DX3sum;
D(N,n) = DX12sum;
E(N,n) = DX123Msum;
F(N,n) = DX123Ssum;

ScalarA(N,n) = DXScalar1sum;
ScalarB(N,n) = DXScalar2sum;
ScalarC(N,n) = DXScalar3sum;
ScalarD(N,n) = DXScalar12sum;
ScalarE(N,n) = DXScalarM123sum;
ScalarF(N,n) = DXScalarS123sum;

ComboA(N,n) = DXCombo1sum;
ComboB(N,n) = DXCombo2sum;
ComboC(N,n) = DXCombo3sum;
ComboD(N,n) = DXCombo12sum;
ComboE(N,n) = DXComboM123sum;
ComboF(N,n) = DXComboS123sum;

end %end t loop
end %end u loop

% In order to achieve an equally weighted average over all possible

```

```

% source directions some weighting factors had to be included. The
% sin (theta) factor accounts for the fact that on a (lat, long)
% grid, such as the (theta, phi) coordinates chosen, there will be
% more functions sampled near the poles than near the equatorial
% plane.
aA(:,:,nn) = A*sth;
aB(:,:,nn) = B*sth;
aC(:,:,nn) = C*sth;
aD(:,:,nn) = D*sth;
aE(:,:,nn) = E*sth;
aF(:,:,nn) = F*sth;

aScalarA(:,:,nn) = ScalarA*sth;
aScalarB(:,:,nn) = ScalarB*sth;
aScalarC(:,:,nn) = ScalarC*sth;
aScalarD(:,:,nn) = ScalarD*sth;
aScalarE(:,:,nn) = ScalarE*sth;
aScalarF(:,:,nn) = ScalarF*sth;

aComboA(:,:,nn) = ComboA*sth;
aComboB(:,:,nn) = ComboB*sth;
aComboC(:,:,nn) = ComboC*sth;
aComboD(:,:,nn) = ComboD*sth;
aComboE(:,:,nn) = ComboE*sth;
aComboF(:,:,nn) = ComboF*sth;

end % End phi loop

end % End theta loop

% Sum the response functions and divide by the respective number of
% components summed. Note the three dimensional matrix must first be summed
% along one axis, then the other.
RTaA = sum(aA,3)/(4*pi*ctheta*cphi*ceps);
RTaB = sum(aB,3)/(4*pi*ctheta*cphi*ceps);
RTaC = sum(aC,3)/(4*pi*ctheta*cphi*ceps);
RTaD = sum(aD,3)/(4*pi*ctheta*cphi*ceps);
RTaE = sum(aE,3)/(4*pi*ctheta*cphi*ceps);
RTaF = sum(aF,3)/(4*pi*ctheta*cphi*ceps);

RTaScalarA = sum(aScalarA,3)/(4*pi*ctheta*cphi*ceps);
RTaScalarB = sum(aScalarB,3)/(4*pi*ctheta*cphi*ceps);
RTaScalarC = sum(aScalarC,3)/(4*pi*ctheta*cphi*ceps);
RTaScalarD = sum(aScalarD,3)/(4*pi*ctheta*cphi*ceps);
RTaScalarE = sum(aScalarE,3)/(4*pi*ctheta*cphi*ceps);
RTaScalarF = sum(aScalarF,3)/(4*pi*ctheta*cphi*ceps);

RTaComboA = sum(aComboA,3)/(4*pi*ctheta*cphi*ceps);
RTaComboB = sum(aComboB,3)/(4*pi*ctheta*cphi*ceps);
RTaComboC = sum(aComboC,3)/(4*pi*ctheta*cphi*ceps);
RTaComboD = sum(aComboD,3)/(4*pi*ctheta*cphi*ceps);
RTaComboE = sum(aComboE,3)/(4*pi*ctheta*cphi*ceps);
RTaComboF = sum(aComboF,3)/(4*pi*ctheta*cphi*ceps);

% Sums along the second axis, and divides by the number of elements summed.
RTaA = sum(RTaA,2)/cc;
RTaB = sum(RTaB,2)/cc;
RTaC = sum(RTaC,2)/cc;
RTaD = sum(RTaD,2)/cc;
RTaE = sum(RTaE,2)/cc;
RTaF = sum(RTaF,2)/cc;

RTaScalarA = sum(RTaScalarA,2)/cc;

```

```

RTaScalarB = sum(RTaScalarB,2)/cc;
RTaScalarC = sum(RTaScalarC,2)/cc;
RTaScalarD = sum(RTaScalarD,2)/cc;
RTaScalarE = sum(RTaScalarE,2)/cc;
RTaScalarF = sum(RTaScalarF,2)/cc;

RTaComboA = sum(RTaComboA,2)/cc;
RTaComboB = sum(RTaComboB,2)/cc;
RTaComboC = sum(RTaComboC,2)/cc;
RTaComboD = sum(RTaComboD,2)/cc;
RTaComboE = sum(RTaComboE,2)/cc;
RTaComboF = sum(RTaComboF,2)/cc;

% End program run time and display in the command prompt.
toc

% Plot one figure to indicate the program has finished running and to
% provide an initial plot to verify results.
a = log10(uu);
figure
plot(a,log10((RTaE')/2))
title ('Averaged Michelson Three Arm Response')

% Save the variable space so additional plots can be generated with the data
% without rerunning the program.
save ('AllSky02MAY');

```

Appendix C

The following MATLAB® code calculates the response functions with respect to gravitational waves originating in the direction of the galactic center.

```
function Z = ThreeDplots ()
% Function that will determine the LISA response for plus, cross, and
% scalar polarizations originating from the galactic center. The resulting
% three dimensional surface plots illustrate the instrument response with
% respect to orbital position and frequency. The program allows for a
% linear combination of cross and plus, and a linear combination of cross
% and scalar polarizations.

% Begin clock to measure the program run-time.
tic

% The perturbation matrices.
hcross = [0 1 0; 1 0 0; 0 0 0];
hplus = [1 0 0; 0 -1 0; 0 0 0];
hscalar = [1 0 0; 0 1 0; 0 0 0];

% The Mixfactor is the coefficient in a linear combination of cross and
% scalar polarizations. For example: Mixfactor = .1 would mean that the
% matrix element of the calculations consists of hx + .1*hs, where hx is
% the matrix element for the cross polarization and hs is the matrix
% element for the scalar polarization.
Mixfactor = .1;

% tstep gives the sample size in days. For example: tstep =1 then the
% response will be calculated for each day of its orbit.
tstep = 2;
tdays = [0:tstep:365];
% Establishes the range of frequencies
uu = 2*pi*(10.^(-4:.01:.4));

% Generates matrices to store values
[r,c] = size (uu);
[rr,cc] = size (tdays);

A = ones(c,cc);
B = A;
C = A;
D = A;
E = A;
F = A;

ScalarA = A;
ScalarB = A;
ScalarC = A;
ScalarD = A;
ScalarE = A;
ScalarF = A;

ComboA = A;
ComboB = A;
ComboC = A;
ComboD = A;
ComboE = A;
ComboF = A;
```

```

% Counting numbers used to designate where data is stored.
n=0;
N=0;

% The values associated with alpha in the LISA frame and store in
% memory for later use. Alpha is the angle between an arm of LISA and the
% x-axis of the LISA frame.
csa1=cos(pi/12);
csa1S=csa1^2;
csa2=cos(5*pi/12);
csa2S=csa2^2;
csa3=cos(3*pi/4);
csa3S=csa3^2;
sna1=sin(pi/12);
sna1S=sna1^2;
sna2=sin(5*pi/12);
sna2S=sna2^2;
sna3=sin(3*pi/4);
sna3S=sna3^2;

% The ranges and step size for epsilon.
epsilonstep = 1/32;
epsilon1 = [(pi*epsilonstep)/2):(pi*epsilonstep):((2/epsilonstep)-1)*pi*...
    (epsilonstep/2)];
[reps,ceps] = size (epsilon1);

% Rotation matrix for theta
RorbitTilt = [1 0 0; 0 cos(pi/3) sin(pi/3); 0 -sin(pi/3) cos(pi/3)];

% Value for theta indicating the direction of the galactic center.
theta = 1.6675;
% Calculates sin and cosine once and stores the values to optimize
% the program.
cth= cos(theta);
sth= sin(theta);

% The rotation matrix for theta. It rotates (pi-theta) about the x
% axis.
RTheta = [1 0 0; 0 cos(pi-theta) sin(pi-theta); 0 -sin(pi-theta) cos(pi-theta)];

% Value for phi indicating the direction of the galactic center.
phi = 4.6572;

% Optimizing the calculations requiring spatial angles theta and phi.
% Mu values are necessary in calculating the time dependant
% component of the the response.
muone= -sth*cos(phi-pi/12);
mutwo= -sth*cos(phi-5*pi/12);
muthree= -sth*cos(phi-3*pi/4);

% The rotation matrix for phi. It rotates pi/2-phi about the
% z axis.
RPhi = [cos(pi/2-phi) sin(pi/2-phi) 0; -sin(pi/2-phi) cos(pi/2-phi) 0; 0 0 1];

% Generating the perturbation matrices in the heliocentric frame through the
% rotations about theta and phi.
hHcross = RPhi'*RTheta'*hcross*RTheta*RPhi;
hHplus = RPhi'*RTheta'*hplus*RTheta*RPhi;
hHscalar = RPhi'*RTheta'*hscalar*RTheta*RPhi;

% The loop used to calculate the response and average over all sky. u = uu
% cycles the calculations for a range of frequencies
for u = uu

```

```

% N is the counting number that controls the storage of response
% function values for each new frequency.
N = N + 1;
% n is the counting number that controls the storage of response
% function values for each new orbital position.
n=0;

% The t loop calculates ans stores the response of the detector for each
% point in its orbit about the sun.
for t = tdays

    % Increment the value of n.
    n=n+1;

    % The rotation matrices that depend upon LISA's orbital position.
    RphiLISA = [cos((t*2*pi)/365) sin((t*2*pi)/365) 0; -sin((t*2*pi)/365)...
                cos((t*2*pi)/365) 0; 0 0 1];
    RbackRotate = [cos(-(t*2*pi)/365) sin(-(t*2*pi)/365) 0; -sin(-(t*2*pi)/365)...
                  cos(-(t*2*pi)/365) 0; 0 0 1];

    % The perturbation matrices calculated in the LISA frame.
    hLcross = RbackRotate*RorbitTilt*RphiLISA*hHcross*RphiLISA'*RorbitTilt'*...
              RbackRotate';
    hLplus = RbackRotate*RorbitTilt*RphiLISA*hHplus*RphiLISA'*RorbitTilt'*...
            RbackRotate';
    hLscalar= RbackRotate*RorbitTilt*RphiLISA*hHscalar*RphiLISA'*RorbitTilt'*...
            RbackRotate';

    % The time independent components associated with each
    % response function evaluated.
    CrossMet1= .5*((hLcross(1,1)*csa1S) + (hLcross(1,2)*csa1*sna1) + ...
                  (hLcross(2,1)*sna1*csa1) + (hLcross(2,2)*sna1S));
    CrossMet2= .5*((hLcross(1,1)*csa2S) + (hLcross(1,2)*csa2*sna2) + ...
                  (hLcross(2,1)*sna2*csa2) + (hLcross(2,2)*sna2S));
    CrossMet3= .5*((hLcross(1,1)*csa3S) + (hLcross(1,2)*csa3*sna3) + ...
                  (hLcross(2,1)*sna3*csa3) + (hLcross(2,2)*sna3S));

    PlusMet1= .5*((hLplus(1,1)*csa1S) + (hLplus(1,2)*csa1*sna1) + ...
                  (hLplus(2,1)*sna1*csa1) + (hLplus(2,2)*sna1S));
    PlusMet2= .5*((hLplus(1,1)*csa2S) + (hLplus(1,2)*csa2*sna2) + ...
                  (hLplus(2,1)*sna2*csa2) + (hLplus(2,2)*sna2S));
    PlusMet3= .5*((hLplus(1,1)*csa3S) + (hLplus(1,2)*csa3*sna3) + ...
                  (hLplus(2,1)*sna3*csa3) + (hLplus(2,2)*sna3S));

    ScalarMet1= .5*((hLscalar(1,1)*csa1S) + (hLscalar(1,2)*csa1*sna1) + ...
                  (hLscalar(2,1)*sna1*csa1) + (hLscalar(2,2)*sna1S));
    ScalarMet2= .5*((hLscalar(1,1)*csa2S) + (hLscalar(1,2)*csa2*sna2) + ...
                  (hLscalar(2,1)*sna2*csa2) + (hLscalar(2,2)*sna2S));
    ScalarMet3= .5*((hLscalar(1,1)*csa3S) + (hLscalar(1,2)*csa3*sna3) + ...
                  (hLscalar(2,1)*sna3*csa3) + (hLscalar(2,2)*sna3S));

    % Resetting variables used in calculating the response
    % function to zero for the next iteration.
    DX1sum=0;
    DX2sum=0;
    DX3sum=0;
    DX12sum=0;
    DX123Msum=0;
    DX123Ssum=0;

    DXScalar1sum=0;
    DXScalar2sum=0;

```

```

DXScalar3sum=0;
DXScalar12sum=0;
DXScalarM123sum=0;
DXScalarS123sum=0;

DXCombo1sum=0;
DXCombo2sum=0;
DXCombo3sum=0;
DXCombo12sum=0;
DXComboM123sum=0;
DXComboS123sum=0;

% Averaging over epsilon accounts for rotation about
% the third Euler angle required in transforming from
% the source frame to the heliocentric frame.
for epsilon = epsilon1

    % Averaging over epsilon accounts for the rotation about the third
    % Euler angle.
    metepsone = cos(2*epsilon)*CrossMet1 - sin(2*epsilon)*PlusMet1;
    metepstwo = cos(2*epsilon)*CrossMet2 - sin(2*epsilon)*PlusMet2;
    metepsthree = cos(2*epsilon)*CrossMet3 - sin(2*epsilon)*PlusMet3;

    ComboCrossScalar1 = metepsone + Mixfactor*ScalarMet1;
    ComboCrossScalar2 = metepstwo + Mixfactor*ScalarMet2;
    ComboCrossScalar3 = metepsthree + Mixfactor*ScalarMet3;

    % Resetting values used in delta loop.
    DX1=0;
    DX2=0;
    DX3=0;
    DX12=0;
    DX123M=0;
    DX123S=0;

    DXScalar1=0;
    DXScalar2=0;
    DXScalar3=0;
    DXScalar12=0;
    DXScalarM123=0;
    DXScalarS123=0;

    DXCombo1=0;
    DXCombo2=0;
    DXCombo3=0;
    DXCombo12=0;
    DXComboM123=0;
    DXComboS123=0;

    % Delta is the phase constant for the incident wave. (kx-wt+delta)
    % This portion of the program finds the amplitude of the response.
    % The response will vary depending upon the initial phase of the
    % gravitational wave. As the program cycles through possible values
    % for the initial phase, it stores the maximum response.
    for delta = pi/32:pi/16:31*pi/32;

        % f1, f2, and f3 include the time dependent parts for the response
        % function.
        f1= ((sin(delta-muone*u)-sin(delta-u))/(u*(1-muone)))+(sin(u+delta)...
            -sin(delta-muone*u))/(u*(1+muone)));
        f2= ((sin(delta-mutwo*u)-sin(delta-u))/(u*(1-mutwo)))+(sin(u+delta)...
            -sin(delta-mutwo*u))/(u*(1+mutwo)));
        f3= ((sin(u*(1+muone)-delta)-sin(mutwo*u-delta))/(u*(1-muthree))...

```



```

        +(sin(u*(1-muone)+delta)+sin(mutwo*u-delta))/(u*(1+muthree)));

% deltaX values correspond to the change in length of
% each arm. This combines the time independent components
% with the time dependent component to achieve the complete
% response of LISA to the gravitational wave.
% X1 corresponds to L1, X2 to L2, and so on.
% Similar calculations were computed for the
% scalar response and the response to the
% combination of scalar and GR polarizations.
deltaX1= metepsone*f1;
deltaX2= metepstwo*f2;
deltaX3= metepsthree*f3;

% In order to calculate the response we must find the delta that
% yields the maximum result (indicating amplitude of response).
if abs(deltaX1) > DX1
    DX1 = abs(deltaX1);
end
if abs(deltaX2) > DX2
    DX2 = abs(deltaX2);
end
if abs(deltaX3) > DX3
    DX3 = abs(deltaX3);
end
if abs(deltaX1-deltaX2) > DX12
    DX12 = abs(deltaX1-deltaX2);
end
if abs(deltaX1+deltaX2-2*deltaX3) > DX123M
    DX123M = abs(deltaX1+deltaX2-2*deltaX3);
end
if abs(deltaX1+deltaX2+deltaX3) > DX123S
    DX123S = abs(deltaX1+deltaX2+deltaX3);
end

deltaXScalar1 = ScalarMet1*f1;
deltaXScalar2 = ScalarMet2*f2;
deltaXScalar3 = ScalarMet3*f3;

if abs(deltaXScalar1) > DXScalar1
    DXScalar1 = abs(deltaXScalar1);
end
if abs(deltaXScalar2) > DXScalar2
    DXScalar2 = abs(deltaXScalar2);
end
if abs(deltaXScalar3) > DXScalar3
    DXScalar3 = abs(deltaXScalar3);
end
if abs(deltaXScalar1-deltaXScalar2)> DXScalar12
    DXScalar12 = abs(deltaXScalar1-deltaXScalar2);
end
if abs (deltaXScalar1+deltaXScalar2-2*deltaXScalar3) > DXScalarM123
    DXScalarM123 = abs (deltaXScalar1+deltaXScalar2-2*deltaXScalar3);
end
if abs (deltaXScalar1+deltaXScalar2+deltaXScalar3) > DXScalarS123
    DXScalarS123 = abs (deltaXScalar1+deltaXScalar2+deltaXScalar3);
end

deltaXCombo1 = ComboCrossScalar1*f1;
deltaXCombo2 = ComboCrossScalar2*f2;
deltaXCombo3 = ComboCrossScalar3*f3;

if abs(deltaXCombo1) > DXCombo1

```

```

        DXCombo1 = abs(deltaXCombo1);
    end
    if abs(deltaXCombo2) > DXCombo2
        DXCombo2 = abs(deltaXCombo2);
    end
    if abs(deltaXCombo3) > DXCombo3
        DXCombo3 = abs(deltaXCombo3);
    end
    if abs(deltaXCombo1-deltaXCombo2)> DXCombo12
        DXCombo12 = abs(deltaXCombo1-deltaXCombo2);
    end
    if abs (deltaXCombo1+deltaXCombo2-2*deltaXCombo3) > DXComboM123
        DXComboM123 = abs (deltaXCombo1+deltaXCombo2-2*deltaXCombo3);
    end
    if abs (deltaXCombo1+deltaXCombo2+deltaXCombo3) > DXComboS123
        DXComboS123 = abs (deltaXCombo1+deltaXCombo2+deltaXCombo3);
    end
end % End delta loop.

% Add the responses for each arm and each combination of arms.
DX1sum = DX1sum + abs(DX1);
DX2sum = DX2sum + abs(DX2);
DX3sum = DX3sum + abs(DX3);
DX12sum = DX12sum + abs(DX12);
DX123Msum = DX123Msum + abs(DX123M);
DX123Ssum = DX123Ssum + abs(DX123S);

DXScalar1sum=DXScalar1sum + abs(DXScalar1);
DXScalar2sum=DXScalar2sum + abs(DXScalar2);
DXScalar3sum=DXScalar3sum + abs(DXScalar3);
DXScalar12sum=DXScalar12sum + DXScalar12;
DXScalarM123sum=DXScalarM123sum + DXScalarM123;
DXScalarS123sum=DXScalarS123sum + DXScalarS123;

DXCombo1sum=DXCombo1sum + abs(DXCombo1);
DXCombo2sum=DXCombo2sum + abs(DXCombo2);
DXCombo3sum=DXCombo3sum + abs(DXCombo3);
DXCombo12sum=DXCombo12sum + DXCombo12;
DXComboM123sum=DXComboM123sum + DXComboM123;
DXComboS123sum=DXComboS123sum + DXComboS123;

end % End epsilon loop

% Stores the sum of the responses for each angle sampled.
A(N,n) = DX1sum;
B(N,n) = DX2sum;
C(N,n) = DX3sum;
D(N,n) = DX12sum;
E(N,n) = DX123Msum;
F(N,n) = DX123Ssum;

ScalarA(N,n) = DXScalar1sum;
ScalarB(N,n) = DXScalar2sum;
ScalarC(N,n) = DXScalar3sum;
ScalarD(N,n) = DXScalar12sum;
ScalarE(N,n) = DXScalarM123sum;
ScalarF(N,n) = DXScalarS123sum;

ComboA(N,n) = DXCombo1sum;
ComboB(N,n) = DXCombo2sum;
ComboC(N,n) = DXCombo3sum;

```

```

        ComboD(N,n) = DXCombo12sum;
        ComboE(N,n) = DXComboM123sum;
        ComboF(N,n) = DXComboS123sum;

    end %end t loop

end %end u loop

% Divide by the number of samples summed to achieve an averaged GR
% polarization (by averaging over epsilon).
A = (1/ceps).*A;
B = (1/ceps).*B;
C = (1/ceps).*C;
D = (1/ceps).*D;
E = (1/ceps).*E;
F = (1/ceps).*F;

ScalarA = (1/ceps).*ScalarA;
ScalarB = (1/ceps).*ScalarB;
ScalarC = (1/ceps).*ScalarC;
ScalarD = (1/ceps).*ScalarD;
ScalarE = (1/ceps).*ScalarE;
ScalarF = (1/ceps).*ScalarF;

ComboA = (1/ceps).*ComboA;
ComboB = (1/ceps).*ComboB;
ComboC = (1/ceps).*ComboC;
ComboD = (1/ceps).*ComboD;
ComboE = (1/ceps).*ComboE;
ComboF = (1/ceps).*ComboF;

% Preparing to generate a loglog plot
bA = log10 (A);
bB = log10 (B);
bC = log10 (C);
bD = log10 (D);
bE = log10 (E);
bF = log10 (F);

bSA=log10 (ScalarA);
bSB=log10 (ScalarB);
bSC=log10 (ScalarC);
bSD=log10 (ScalarD);
bSE=log10 (ScalarE);
bSF=log10 (ScalarF);

bCA = log10 (ComboA);
bCB = log10 (ComboB);
bCC = log10 (ComboC);
bCD = log10 (ComboD);
bCE = log10 (ComboE);
bCF = log10 (ComboF);

% Generate a plot to signify the program has finished running and allow the
% user to verify an initial set of the results.
figure
surf (bA)

% End program run time and display in the command prompt.
toc
% Saves variables for reference eliminating the need to run the program more
% then once for a set of values.
save ('ThreeDplots31MAR');

```

References

- [1] B. F. Schutz, *A First Course in General Relativity*, Cambridge, England: Cambridge University Press, 1985.
- [2] E. F. Taylor and J. A. Wheeler, *Spacetime Physics*, San Francisco: W. H. Freeman and Company, 1963.
- [3] C. Brans and R. H. Dicke, *Mach's Principle and a Relativistic Theory of Gravitation*, Phys. Rev. 124:925-935. (1961)
- [4] C. Will, *Gravitational Radiation and the Validity of General Relativity*, Phys. Today 52, 38 – 43 (October 1999).
- [5] P. Scharre and C. M. Will, *Testing Scalar-Tensor Gravity using Space Gravitational-Wave Interferometers*, Phys. Rev. D 65, 042002 (2002)
- [6] Hawking, Stephen W. and Israel, Werner (Eds.). *General Relativity: An Einstein Centenary Survey*. Cambridge, England: Cambridge University Press, 1979.
- [7] P. Bender *et al.*, *LISA Pre-Phase A Report (Second Edition)* (1998) (unpublished). Available at: <http://www.srl.caltech.edu/lisa/documents/PrePhaseA.pdf>
- [8] J. Foster and J. D. Nightingale, *A Short Course in General Relativity*, New York: Springer-Verlag, 1995.
- [9] E. D. Black and R. N. Gutenkunst, *An introduction to signal extraction in interferometric gravitational wave detectors*, American Journal of Physics 71(4), 365-378 (April 2003)
- [10] *LISA Pictures and Animations*, <http://www.srl.caltech.edu/lisa/> (25 Mar. 2004).
- [11] S.L. Larson, W.A. Hiscock, R.W. Hellings, *Sensitivity Curves for Spaceborne Gravitational Wave Interferometers*, Phys. Rev. D 67 062001 (2003)
- [12] R. Schilling, *Angular and Frequency Response of LISA*, Class. Quantum Grav. 14 1513–1519 (1997)